Atmos. Chem. Phys. Discuss., 15, 17887–17943, 2015
www.atmos-chem-phys-discuss.net/15/17887/2015/
doi:10.5194/acpd-15-17887-2015

Atmospheric Chemistry and Physics Discussions
Open Access

The contribution of oceanic halocarbons to marine and free troposphere air over the tropical West Pacific

S. Fuhlbrügge[1], B. Quack[1], S. Tegtmeier[1], E. Atlas[2], H. Hepach[1], Q. Shi[3], S. Raimund[1], and K. Krüger[4]

[1]GEOMAR, Helmholtz Centre for Ocean Research Kiel, Kiel, Germany
[2]Rosenstiel School for Marine and Atmospheric Sciences, Miami, FL, USA
[3]Department of Oceanography – Dalhousie University, Halifax, Canada
[4]University of Oslo, Oslo, Norway

Received: 26 March 2015 – Accepted: 11 June 2015 – Published: 02 July 2015

Correspondence to: K. Krüger (kirstin.krueger@geo.uio.no)

Published by Copernicus Publications on behalf of the European Geosciences Union.

Abstract

Emissions of halogenated very short lived substances (VSLS) from the tropical oceans contribute to the atmospheric halogen budget and affect tropospheric and stratospheric ozone. Here we investigate the contribution of natural oceanic VSLS emissions to the Marine Atmospheric Boundary Layer (MABL) and their transport into the Free Troposphere (FT) over the tropical West Pacific. The study concentrates in particular on ship and aircraft measurements of the VSLS bromoform, dibromomethane and methyl iodide and meteorological parameters during the SHIVA (Stratospheric Ozone: Halogen Impacts in a Varying Atmosphere) campaign in the South China and Sulu Seas in November 2011. Elevated oceanic concentrations of 19.9 (2.80–136.91) $\mathrm{pmol\,L^{-1}}$ for bromoform, 5.0 (2.43–21.82) $\mathrm{pmol\,L^{-1}}$ for dibromomethane and 3.8 (0.55–18.83) $\mathrm{pmol\,L^{-1}}$ for methyl iodide in particular close to Singapore and at the coast of Borneo with high corresponding oceanic emissions of $1486 \pm 1718\,\mathrm{pmol\,m^{-2}\,h^{-1}}$ for bromoform, $405 \pm 349\,\mathrm{pmol\,m^{-2}\,h^{-1}}$ for dibromomethane and $433 \pm 482\,\mathrm{pmol\,m^{-2}\,h^{-1}}$ for methyl iodide characterize this tropical region as a strong source of these compounds. Unexpectedly atmospheric mixing ratios in the MABL were relatively low with 2.08 ± 2.08 ppt for bromoform, 1.17 ± 1.17 ppt for dibromomethane and 0.39 ± 0.09 ppt for methyl iodide. We use meteorological and chemical ship and aircraft observations, FLEXPART trajectory calculations and source-loss estimates to identify the oceanic VSLS contribution to the MABL and to the FT. Our results show that a convective, well-ventilated MABL and intense convection led to the low atmospheric mixing ratios in the MABL despite the high oceanic emissions in coastal areas of the South-China and Sulu Seas. While the accumulated bromoform in the FT above the region origins almost entirely from the local South China Sea area, dibromomethane is largely advected from distant source regions. The accumulated FT mixing ratio of methyl iodide is higher than can be explained with the local oceanic or MABL contributions. Possible reasons, uncertainties and consequences of our observations and model estimates are discussed.

1 Introduction

The contribution of halogens to the atmospheric ozone chemistry is well known. Besides the destruction of stratospheric ozone (Solomon, 1999), halogen radicals (chlorine, bromine, iodine) also affect tropospheric ozone chemistry (Saiz-Lopez and von Glasow, 2012). Halogen radicals are released via photochemical and heterogeneous reaction cycles from organic halogenated trace gases originating from anthropogenic and natural sources, including macro algae, seaweed, phytoplankton and other marine biota. A large number of very short lived brominated and iodinated organic substances are emitted from tropical oceans and coastal regions to the atmosphere (Gschwend et al., 1985; Carpenter and Liss, 2000; Quack and Wallace, 2003; Quack et al., 2007; Liu et al., 2013). In particular, marine emissions of bromoform ($CHBr_3$), dibromomethane (CH_2Br_2) and methyl iodide (CH_3I) are major contributors of organic bromine and iodine to the atmosphere (Montzka and Reimann, 2011). Mean atmospheric lifetimes of the halogenated very short lived substances (VSLS) are 26 days for bromoform, 120 days for dibromomethane (Ko et al., 2003) and 4 days for methyl iodide (Solomon et al., 1994). Climate change could strongly affect marine biota and thereby halogen sources and the oceanic emission strength (Hepach et al., 2014).

Aircraft measurements from Dix et al. (2013) suggest that the halogen-driven ozone loss in the Free Troposphere (FT) is currently underestimated. In particular, significant elevated amounts of the iodine oxide free radical (IO) were found in the FT over the Central Pacific suggesting that iodine has a much larger effect on the FT ozone budget than currently estimated by chemical models. Coinciding with this study, Tegtmeier et al. (2013) projected a higher methyl iodide delivery to the Upper Troposphere/Lower Stratosphere (UTLS) over the tropical West Pacific than previously reported, using an observation based emission climatology by Ziska et al. (2013). Significantly lower amounts of tropospheric and stratospheric ozone are found in chemistry-transport and chemistry climate model runs when taking atmospheric bromine into account (von Glasow et al., 2004; Yang et al., 2005, 2014). Even though the influence of halogens on the tropospheric and stratospheric ozone chemistry is crucial, halogen sources and transport ways are still not fully understood. Deep tropical convective events (Aschmann et al., 2011; Tegtmeier et al., 2013; Carpenter et al., 2014) as well as tropical cyclones, i.e. typhoons (Tegtmeier et al., 2012) are projected to transport the VSLS rapidly from the ocean surface to the upper tropical tropopause layer. The tropical West Pacific is an intense source region for VSLS (Krüger and Quack, 2013). However, only low mean atmospheric mixing ratios were observed for VSLS in the Eastern and Southeast China Seas during ship cruises in 1994 and 2009 (Yokouchi et al., 1997; Quack and Suess, 1999) and through the tropical West Pacific in 2010 (Quack et al., 2011; Brinckmann et al., 2012). None of these previous studies investigated the contribution of oceanic VSLS emissions to the marine atmospheric boundary layer (MABL) and to the FT in this hot spot region with large oceanic sources and strong convective activity.

The SHIVA ("Stratospheric Ozone: Halogen Impacts in a Varying Atmosphere") ship, aircraft and ground-based campaign during November and December 2011 in the Southern South China and Sulu Seas investigated oceanic emission strengths of marine VSLS, as well as their atmospheric transport and chemical transformation from the ocean surface to the upper troposphere. The goal of SHIVA was to improve the prediction of rate, timing and sensitivity of the ozone layer recovery due to climate forcing by combining observations and models. For more details about the SHIVA campaign see the ACP special issue (http://www.atmos-chem-phys.net/special_issue306.html).

In this study, we present campaign data from the research vessel (R/V) *SONNE* and the research aircraft (R/A) *FALCON*. We identify the contribution of oceanic emissions to the MABL and their exchange into the FT applying in-situ observations, trajectory calculations and source-loss estimates. The results are crucial for a better process understanding and for chemical transport model validation (Hossaini et al., 2013; Aschmann and Sinnhuber, 2013). An overview of the data and the methods used in this study is given in Sect. 2. Section 3 provides results from the meteorological observations along the cruise. Section 4 compares atmospheric VSLS measurements derived on R/V *SONNE* and R/A *FALCON* by different gas chromatographic/mass spectromet-

ACPD
15, 17887–17943, 2015

ric (GC/MS) instruments. The contribution of the oceanic emissions to the MABL and FT air is investigated and discussed in Sect. 5 by applying model calculations and the field observations. Finally, a summary of the results is given in Sect. 6.

2 Data and methods

2.1 SHIVA SONNE

2.1.1 Ship cruise

The cruise of R/V *SONNE* started on 15 November 2011 in Singapore and ended on 29 November 2011 in Manila, Philippines (Fig. 1a). The ship crossed the southwest South China Sea towards the northwest coast of Borneo from 16–19 November 2011. From 19–23 November 2011 the ship headed northeast along the northern coast of Borneo towards the Sulu Sea. Two diurnal stations took place on 18 November 2011 at 2.4° N/110.6° E and on 22 November 2011 at 6.0° N/114.8° E. Two meetings between R/V *SONNE* and R/A *FALCON* were carried out on 19 and 21 November 2011, where R/A *FALCON* passed R/V *SONNE* within a distance of about 100 m for several times to get simultaneous measurements of the same air masses. On 24 November 2011 the ship entered the Sulu Sea, and after 4 days transect, R/V *SONNE* reached the Philippine coast.

2.1.2 Aircraft campaign

16 measurement flights were carried out with R/A *FALCON* between 16 November and 11 December 2011 as part of the SHIVA campaign to investigate halogenated VSLS from the surface up to 13 km altitude over the South China and Sulu Seas. Observations were performed between 1 and 8° N, as well as 100 and 122° E, using Miri, Borneo (Malaysia) as the aircraft base. A detailed description of the VSLS measurements and flight tracks can be found in Sala et al. (2014).

Discussion Paper | Discussion Paper | Discussion Paper | Discussion Paper |
ACPD
15, 17887–17943, 2015

2.2 Meteorological observations during SHIVA

2.2.1 Measurements onboard R/V *SONNE*

Meteorological parameters (temperature, air pressure, humidity and wind) were recorded at 20 m height every second on R/V *SONNE*. A 10 min running mean of this data is used for our investigations. An optical disdrometer ("ODM-470") measured the amount and intensity of precipitation during the cruise at 15 m height every minute. To obtain atmospheric profiles of air temperature, relative humidity and wind from the surface to the stratosphere 67 GRAW DFM-09 and 6 GRAW DFM-97 radiosondes were launched every 6 h at standard UTC times (00:00, 06:00, 12:00, 18:00) from the working deck of R/V *SONNE* at about 2 m a.s.l. At the 24 h stations, the launch frequency was increased to 2–3 h to analyse short term diel variations of the atmospheric boundary layer. During the cruise the radiosonde data was integrated in near real time into the Global Telecommunication System (GTS) to improve meteorological reanalyses such as ERA-Interim, which is used as input data for the trajectory calculations (Sect. 5).

2.2.2 Marine atmospheric boundary layer

The MABL is the atmospheric surface layer above the ocean in which trace gas emissions are mixed vertically by convection and turbulence on short time scales of about an hour (Stull, 1988; Seibert et al., 2000). The upper boundary of the MABL is either limited by a stable layer e.g. a temperature inversion or by a significant reduction in air moisture. Determination of the MABL height can be achieved by theoretical approaches, e.g. using critical Bulk Richardson number (Troen and Mahrt, 1986; Vogelezang and Holtslag, 1996; Sorensen, 1998) or by practical approaches summarized in Seibert et al. (2000). An increase with height of the virtual potential temperature, the temperature an air parcel would acquire if adiabatically brought to standard pressure with regard to the humidity of the air parcel, identifies the base of the stable layer, which is typically found between 100 m and 3 km altitude (Stull, 1988). In this study, we use the height of the base of the stable layer increased by half of the stable layer depth as definition for the MABL height. The height of the MABL is determined from the atmospheric profiles measured by radiosondes launched on board the ship, as described in detail by Fuhlbrügge et al. (2013).

2.2.3 Convective energy

Intense solar insolation and high sea surface temperatures (SST) favour the South China and Sulu Seas for high convective activity. To indicate atmospheric instabilities that can lead to convective events the convective available potential energy (CAPE) (Margules, 1905; Moncrieff and Miller, 1976) is calculated. CAPE is defined as the cumulative buoyant energy of an air parcel from the level of free convection (LFC), the level where the environmental temperature decreases faster than the moist adiabatic lapse rate of a saturated air parcel at the same level, and the equilibrium level (EL), the height at which the air parcel has the same temperature as the environment. CAPE is computed after Eq. (1), with g as the gravitational constant, $T_{\mathrm{v,\,p}}$ as the virtual temperature of an adiabatic ascending air parcel at geometric height z, $T_{\mathrm{v,\,e}}$ as the virtual temperature of the environment at z, z_{LFC} as the height of the level of free convection and z_{EL} as the height of the equilibrium level. CAPE can range from 0 to more than $3\,\mathrm{kJ\,kg^{-1}}$ for very intense thunderstorms (Thompson and Edwards, 2000).

$$\mathrm{CAPE} = \int_{z_{\mathrm{LFC}}}^{z_{\mathrm{EL}}} g \cdot \left(\frac{T_{\mathrm{v,\,p}} - T_{\mathrm{v,\,e}}}{T_{\mathrm{v,\,e}}} \right) \mathrm{d}z \tag{1}$$

2.3 VSLS measurements and flux calculation

For the investigation of VSLS abundances, marine surface air and sea water were sampled synchronously on R/V *SONNE* along the cruise track. From these measurements the oceanic emissions of the compounds during the SHIVA campaign were calculated

ACPD
15, 17887–17943, 2015

(Sect. 2.3.3). Additionally, VSLS abundances in the MABL and the FT were measured by R/A *FALCON*.

2.3.1 Atmospheric samples

Air samples were taken on a 3 hourly basis along the cruise track, and in a 1–2 hourly rhythm during the 24 h stations on R/V *SONNE* resulting in a total of 195 samples during the cruise. The air was pressurized to 2 atm in pre-cleaned stainless steel canisters using a metal bellows pump. The samples were analyzed within 6 months after the cruise at the Rosenstiel School for Marine and Atmospheric Sciences (RSMAS, Miami, Florida) according to Schauffler et al. (1999) with an instrumental precision of ∼ 5 %. Further details on the precision and the preparation of the samples and the use of standard gases are described in Montzka et al. (2003) and Fuhlbrügge et al. (2013). On R/A *FALCON* ambient air was analysed in situ by a GhOST-MS (Gas Chromatograph for the Observation of Stratospheric Tracers – coupled with a Mass Spectrometer) by the Goethe University of Frankfurt (GUF). Additionally 700 mL glass flasks were filled with ambient air to a pressure of 2.5 bar with a diaphragm pump using the R/A *FALCON* whole air sampler (WASP) and analysed within 48 h by a ground-based gas chromatography – mass spectrometry (GC/MS) instrument (Agilent 6973) of the University of East Anglia (Worton et al., 2008). During the flights GhOST measurements were conducted approximately every 5 min with a sampling time of 1 min, while WASP samples were taken every 3–15 min with a sampling time of 2 min. Further details on the instrumental precision, intercalibration of both instruments and observations on R/A *FALCON* are given in Sala et al. (2014). Given that the ground-based GC/MS investigated only brominated compounds, methyl iodide data is not available from WASP. Measurements from R/V *SONNE* and R/A *FALCON* were calibrated both with NOAA standards.

ACPD
15, 17887–17943, 2015

2.3.2 Water samples

Sea water samples for dissolved VSLS were taken in-situ on a 3 hourly basis from the moon pool of R/V *SONNE* at a depth of 5 m from a continuously working water pump. Measurements were interrupted between 16 November, 00:00 UTC to 17 November 2011 12:00 UTC due to permission issues in the southwest South China Sea. For the analysis of the water samples, a purge and trap system was attached to a gas chromatograph with mass spectrometric detection in single-ion mode with a precision of 10 % determined from duplicates. The approach is described in detail by Hepach et al. (2014).

2.3.3 Sea–air flux

The sea–air flux (F) of bromoform, dibromomethane and methyl iodide is calculated with k_w as specific transfer coefficient of the compound and Δc as the concentration gradient between the specific water and atmospheric concentrations (Eq. 2). For the determination of k_w, the air–sea gas exchange parameterization of Nightingale et al. (2000) was used and a Schmidt number (Sc) correction to the carbon dioxide derived transfer coefficient k_{CO_2} after Quack and Wallace (2003) was applied for the three gases (Eq. 3).

$$F = k_w \cdot \Delta c \quad (2)$$

$$k_w = k_{CO_2} \cdot \frac{Sc^{-\frac{1}{2}}}{600} \quad (3)$$

Details on deriving the air–sea concentration gradient are further described in Hepach et al. (2014) and references therein.

Discussion Paper | Discussion Paper | Discussion Paper | Discussion Paper |
ACPD
15, 17887–17943, 2015
The contribution of oceanic halocarbons to marine and free troposphere air
S. Fuhlbrügge et al.
Title Page
Abstract Introduction
Conclusions References
Tables Figures
◀ ▶
Back Close
Full Screen / Esc
Printer-friendly Version
Interactive Discussion

2.4 Oceanic VSLS contribution to the MABL and FT

2.4.1 Trajectory calculations

For the determination of the air mass transport from the surface to the FT the Lagrangian Particle Dispersion Model FLEXPART of the Norwegian Institute for Air Research in the Department of Atmospheric and Climate Research (Stohl et al., 2005) was used. The model has been extensively evaluated in earlier studies (Stohl et al., 1998; Stohl and Trickl, 1999) and includes parameterizations for turbulence in the atmospheric boundary layer and the FT as well as moist convection (Stohl and Thomson, 1999; Forster et al., 2007). Meteorological input fields are retrieved from the ECMWF (European Centre for Medium-Range Weather Forecasts) assimilation reanalysis product ERA-Interim (Dee et al., 2011) with a horizontal resolution of $1^{\circ} \times 1^{\circ}$ and 60 vertical model levels. The ship-based radiosonde measurements (Sect. 2.2.1) were assimilated into ERA-Interim data. The 6 hourly input fields provide air temperature, horizontal and vertical wind, boundary layer height, specific humidity, as well as convective and large scale precipitation. For the trajectory analysis, 80 release points were defined along the cruise track. Time and position of these release events are synchronized with the water and air samples (Sect. 2.3). At these releases, 10 000 trajectories were launched per release point from the ocean surface within a time frame of ±30 min and an area of $\sim 500\,\mathrm{m}^2$.

2.4.2 VSLS source-loss estimate in the MABL

A VSLS source-loss estimate for the MABL over the South China and Sulu Seas is obtained by applying the mass balance principle to the oceanic emissions, and to the time scales of air mass transport from FLEXPART and chemical loss. For each release event we define a box of the size given by the in-situ height of the MABL and by the horizontal area of the trajectory releases ($\sim 400\,\mathrm{m}^2$ centred on the measurement location). Our VSLS source-loss estimate is based on a steady-state assumption of a constant

VSLS mixing ratio (given by the atmospheric measurements) within this box. The average VSLS delivery and loss calculated for these boxes is denoted as MABL source-loss estimate in this manuscript.

To derive the amount of VSLS delivery to the MABL by oceanic emissions, we consider the specific sea–air flux constant during each trajectory release and the emissions homogeneously distributed in the MABL. The contribution of the sea–air flux to the MABL concentrations of the specific compounds is defined as the Oceanic Delivery (OD). The OD is calculated as the ratio of the VSLS flux out of the ocean (in mol per day) and the total amount of the VSLS in the box (in mol) with the latter derived from the box dimensions and the measured VSLS mixing ratio, given in percentage per day. Another important process determining the VSLS concentrations in the MABL is the loss of MABL air to the FT caused by vertical transport, defined here as COnvective Loss (COL). This loss process is calculated from the mean residence time of the FLEXPART trajectories in the observed MABL during each release, is given as a negative number in percentage per day and equals the loss of VSLS from the MABL to the FT. Chemical loss processes in form of reaction with OH and photolysis can be described by the chemical lifetime of the VSLS in the MABL. Based on tropical MABL lifetime estimates of 16 days for bromoform, 60 days for dibromomethane (Hossaini et al., 2010) and 3 days for methyl iodide (R. Hossaini, personal communication, 2013) the Chemical Loss (CL) is estimated in percentage per day and given as a negative quantity.

Relating the delivery of VSLS from the ocean to the MABL (OD) and the loss of MABL air with the contained VSLS to the FT (COL) results in an Oceanic Delivery Ratio (ODR) (Eq. 4):

$$\mathrm{ODR} = \frac{\mathrm{OD}\,[\%\,\mathrm{day}^{-1}]}{-\mathrm{COL}\,[\%\,\mathrm{day}^{-1}]} = \frac{\text{Sea–Air flux contribution }[\%\,\mathrm{day}^{-1}]}{\text{Loss of MABL air to the FT }[\%\,\mathrm{day}^{-1}]} \tag{4}$$

ACPD
15, 17887–17943, 2015

Similarly, we relate the Chemical Loss in the MABL (CL) to the MABL VSLS loss into the FT (COL) to derive a Chemical Loss Ratio (CLR) (Eq. 5):

$$\mathrm{CLR} = \frac{\mathrm{CL}\ [\%\,\mathrm{day}^{-1}]}{-\mathrm{COL}\ [\%\,\mathrm{day}^{-1}]} = \frac{\text{Loss through chemistry}\ [\%\,\mathrm{day}^{-1}]}{\text{Loss of MABL air to the FT}\ [\%\,\mathrm{day}^{-1}]} \quad (5)$$

Assuming steady state in the box, the oceanic delivery, chemical loss and loss to the FT must be balanced by advective transport of air masses in and out of the box. We define the change of the VSLS through advective transport as Advective Delivery (AD) in percentage per day (Eq. 6). Additionally, we define the ratio of change in VSLS caused by advection (AD) to the loss of VSLS out of the MABL to the FT as Advective Delivery Ratio (ADR) in Eq. (7):

$$\mathrm{AD} = -\mathrm{COL} - \mathrm{CL} - \mathrm{OD} \quad (6)$$

$$\mathrm{ADR} = \frac{\mathrm{AD}\ [\%\,\mathrm{day}^{-1}]}{-\mathrm{COL}\ [\%\,\mathrm{day}^{-1}]} = 1 - \mathrm{CLR} - \mathrm{ODR} \quad (7)$$

Note that for the VSLS within the MABL box, COL and CL are loss processes and given as negative numbers while OD and AD (besides a very few exceptions for the latter) are source processes and given as positive numbers. In order to derive the ratios, we have divided CL, OD and AD by −COL and therefore end up with negative ratios for the loss process and positive ratios for the source processes.

In a final step, we relate the source-loss ratios (ODR, CLR and ADR) to the MABL VSLS volume mixing ratio ($\mathrm{VMR_{MABL}}$) in the box (Eq. 8–10), to derive information on the different contributions to the observed mixing ratio. Assuming steady state in the box and a complete loss of all air masses into the FT, we want to estimate how much of newly supplied VSLS results from oceanic delivery ($\mathrm{VMR_{ODR}}$), how much is destroyed

ACPD
15, 17887–17943, 2015

by chemistry (VMR_{CLR}) and how much results from advective transport (VMR_{ADR}).

$$VMR_{ODR} = ODR \cdot VMR_{MABL} \quad (8)$$

$$VMR_{CLR} = CLR \cdot VMR_{MABL} \quad (9)$$

$$VMR_{ADR} = ADR \cdot VMR_{MABL} \quad (10)$$

2.4.3 Oceanic and MABL VSLS contribution to the FT

The cruise covered heterogeneous oceanic regions in the South China Sea. We use a simplified approach to calculate the mean contribution of boundary layer air masses observed on the ship and the oceanic compounds therein to the FT above the South China and Sulu Seas. The contribution is determined as a function of time and altitude based on the distribution of the trajectories released at each measurement location along the ship track. According to R/A *FALCON* observations and our trajectory calculations we assume a well mixed FT within 5° S–20° N, 100–125° E. Observations on R/V *SONNE*, on the other hand, are characterized by large variability and are considered to be representative for the area along the cruise track where the VSLS were measured in the water and atmosphere. We constrain our calculations to this area and define 80 vertical columns along the cruise track. Each column extends horizontally over the area given by the starting points of the trajectories (20 m × 20 m centred on the measurement location) and vertically from the sea surface up to the highest point of R/A *FALCON* observations around 13 km altitude. For each of the 80 trajectory releases along the cruise track, 10 000 trajectories were launched and assigned an identical MABL air parcel containing air with the VSLS mixing ratios observed on R/V *SONNE* during the time of the trajectory release. The volume of the air parcel is given by the in-situ height of the MABL and the horizontal extend of the release box (20 m × 20 m) divided by 10 000 trajectories. The transport of the MABL air parcels is specified by the trajectories, assuming that no mixing occurs between the parcels during the transport. Chemical loss of the VSLS in each air parcel is taken into account through chemical degradation according to their specific tropospheric lifetimes. We average over the volume and mixing ratios of all trajectories within the South China Sea area independent of their exact horizontal location. Since the VSLS mixing ratios in the FT from the aircraft measurements are representative for the whole South China Sea area, it is for our approach not important where the air parcels reside within this area. Only if trajectories leave the South China Sea area they are not taken into account any longer. Due to the decreasing density of air in the atmosphere with height, the volume of the MABL air parcels expands along the trajectories with increasing altitude. The expanding MABL air parcels take up an increasing fraction of air within the FT column, which is taken into account in our calculations using density profiles from our radiosonde measurements.

We calculate the contribution of oceanic compounds to the FT for 25 layers of 500 m height intervals, situated between 0.5 and 13 km altitude within the column above the measurement location. For each layer, the ratio r_{MABL} of the volume of the MABL air parcels with the VSLS mixing ratio $\mathrm{VMR}_{\mathrm{MABL}}$ to the whole air volume of the layer is calculated. The ratio of advected FT air with a mixing ratio $\mathrm{VMR}_{\mathrm{AFT}}$ to the whole air volume of the layer is r_{AFT} respectively, with $r_{\mathrm{MABL}} + r_{\mathrm{AFT}} = 1$. In our simulation, the FT air with a mixing ratio $\mathrm{VMR}_{\mathrm{FT}}$ observed by R/A *FALCON* at a specific height is composed of the MABL air parcels and of the advected FT air parcels (Eq. 11):

$$r_{\mathrm{MABL}} \cdot \mathrm{VMR}_{\mathrm{MABL}} + r_{\mathrm{AFT}} \cdot \mathrm{VMR}_{\mathrm{AFT}} = (r_{\mathrm{MABL}} + r_{\mathrm{AFT}}) \cdot \mathrm{VMR}_{\mathrm{FT}} \quad (11)$$

The relative Contribution C_{MABL} of VSLS observed in the MABL to the VSLS observed in the FT is computed in altitude steps of 500 m (Eq. 12):

$$C_{\mathrm{MABL}}[\%] = 100 \cdot (r_{\mathrm{MABL}} \cdot \mathrm{VMR}_{\mathrm{MABL}})/\mathrm{VMR}_{\mathrm{FT}} \quad (12)$$

The oceanic Contribution C_{ODR} of the South China Sea to the atmospheric mixing ratios in the FT is computed after Eq. (13):

$$C_{\mathrm{ODR}}[\%] = 100 \cdot (r_{\mathrm{MABL}} \cdot \mathrm{VMR}_{\mathrm{ODR}})/\mathrm{VMR}_{\mathrm{FT}} \quad (13)$$

The simplified approach also allows us to derive mean VSLS mixing ratios accumulated in the FT from both MABL VSLS and oceanic emissions. The FT VSLS mixing ratios are

ACPD
15, 17887–17943, 2015

simulated for each of the 80 releases by initiating a new trajectory release using same meteorological conditions and VSLS MABL observations, when the former MABL air has been transported into the FT, according to the specific residence time in the MABL. The initial FT background mixing ratios are 0 ppt for each VSLS. The accumulated mean mixing ratio of a compound at a specific height is then computed after Eq. (14):

$$\mathrm{VMR}_{\mathrm{MFT}} = r_{\mathrm{MABL}_1} \cdot \mathrm{VMR}_{\mathrm{MABL}_1} + r_{\mathrm{MABL}_2} \cdot \mathrm{VMR}_{\mathrm{MABL}_2} + \ldots + r_{\mathrm{MABL}_i} \cdot \mathrm{VMR}_{\mathrm{MABL}_i} \quad (14)$$

Here, $\mathrm{VMR}_{\mathrm{MFT}}$ is the modelled accumulated FT mixing ratio, r_{MABL_i} is the ratio of MABL air parcels in 20 m × 20 m × 500 m layers between 0.5 and 13 km altitude to the total volume of each layer, $\mathrm{VMR}_{\mathrm{MABL}_i}$ is the mixing ratio in the MABL air parcels including chemical degradation since release from the MABL, i is the number of initiated runs per release. A steady state for the compounds is reached, when variations in their mixing ratios vary less than 1 % between two initiated runs. For bromoform the steady state is reached after 11.0 ± 2.1 days (mean ± σ), 11.8 ± 2.4 days for dibromomethane and 8.0 ± 1.4 days for methyl iodide. The overall mean FT mixing ratio in the South China Sea is derived as the mean from the 80 individually calculated FT mixing ratios determined along the cruise. The oceanic contribution to the FT compounds is calculated with $\mathrm{VMR}_{\mathrm{ODR}}$ from Eq. (8) inserted as $\mathrm{VMR}_{\mathrm{MABL}}$ in Eq. (14).

3 Meteorological conditions in the MABL and the FT

3.1 Meteorology along the ship cruise

Moderate to fresh trade winds are dominating the South China and Sulu Seas (Fig. 1a and b), which is reflected by the overall mean wind direction of northeast (50–60°) and a mean wind speed of $5.5 \pm 2.9\,\mathrm{m\,s^{-1}}$ during the cruise. The wind observations reveal two different air mass origins. Between 15 and 19 November 2011 a gentle mean wind speed of $3.7 \pm 1.8\,\mathrm{m\,s^{-1}}$ with a *northern* wind direction was observed, influenced by a weak low pressure system (not shown here) over the central South China

ACPD
15, 17887–17943, 2015

Sea moving southwest and passing the ship position on 17 November 2011. During 20–29 November 2011 the wind direction changed to *northeast* and the mean wind speed increased to moderate $6.4 \pm 3.0\,\mathrm{m\,s^{-1}}$. A comparison between 6 hourly ERA-Interim wind and a 6 hourly averaged mean of the observed wind on R/V *SONNE* reveals an underestimation of the wind speed by ERA-Interim along the cruise track by $1.6 \pm 1.4\,\mathrm{m\,s^{-1}}$ on average (not shown here). The mean deviation of the wind direction between reanalysis and observation is $2 \pm 37^{\circ}$. Reanalysis and observed wind speeds correlate with $R = 0.76$ and the wind directions with $R = 0.86$, reflecting a good overall agreement between ship observation and ERA-Interim winds. With an observed mean surface air temperature (SAT) of $28.2 \pm 0.8\,^{\circ}\mathrm{C}$ and a mean SST of $29.1 \pm 0.5\,^{\circ}\mathrm{C}$ the SAT is on average $1.0 \pm 0.7\,^{\circ}\mathrm{C}$ below the SST, which benefits convection of surface air (Fig. 2).

3.2 CAPE and humidity

The mean CAPE computed from the radiosonde data is $998 \pm 630\,\mathrm{J\,kg^{-1}}$ and typically elevated for tropical regions (Fig. 3). Highest CAPE during the cruise was observed on 16 November 2011 at 12:00 UTC in the southern South China Sea and exceeded $2.9\,\mathrm{kJ\,kg^{-1}}$, revealing developing convection. ERA-Interim mean CAPE during the cruise was $825 \pm 488\,\mathrm{J\,kg^{-1}}$ and about $170\,\mathrm{J\,kg^{-1}}$ lower than observed by the radiosondes.

Precipitation measurements by the optical disdrometer ODM-470 are shown in Fig. 3. Besides a number of small rain events during the cruise, three major convective rain events are evident on 16, 21, and 24 November 2011. The total amount of accumulated rain during the cruise was 52.3 mm. The most intense rain rate of $16.3\,\mathrm{mm\,h^{-1}}$ was observed on 16 November 2011 in the southwest South China Sea. The relatively low total precipitation during the cruise is reflected by negative precipitation anomalies in November 2011 compared to the long term climate mean along the northern coast of Borneo (Climate Diagnostics Bulletin, November 2011, Climate Prediction Center).

Figure 4 shows the time series of the relative humidity measured by the radiosondes launched on R/V *SONNE* from the surface up to the mean height of the cold point tropopause at 17 km. Increased relative humidity within the lower troposphere coincides with the rain fall events observed by the disdrometer on 16, 21, and 24 November 2011 (compare with Fig. 3). Elevated humidity is found on average up to about 6 km, which implies a distinct transport of water vapour to the mid troposphere during the cruise by deep convection or advection of humid air from a nearby convective cell.

3.3 Marine atmospheric boundary layer

Higher SSTs than SATs (Fig. 2) cause unstable atmospheric conditions (negative values) between the surface and about 50–100 m height (Fig. 5). Surface air is heated by warmer surface waters and is enriched with humidity both benefiting moist convection. The stability of the atmosphere increases above 420 ± 120 m and indicates the upper limit of the MABL at this altitude range derived from radiosonde data (Fig. 5). The ERA-Interim MABL height along the cruise track is with 560 ± 130 m systematically higher, but still within the upper range of the MABL height derived from the radiosonde measurements. The unstable conditions of the MABL and the increase of the atmospheric stability above the MABL reflect the characteristics of a convective well ventilated tropical boundary layer. In contrast to cold oceanic upwelling regions with a stable and isolated MABL (Fuhlbrügge et al., 2013), the vertical gradient of the relative humidity measured by the radiosondes (Sect. 3.1) and the height of the MABL do not coincide. This is caused by increased mixing through and above the MABL by turbulence and convection, which leads to the well-ventilated convective MABL.

ACPD
15, 17887–17943, 2015

4 Atmospheric VSLS over the South China and Sulu Seas

4.1 Atmospheric surface observations on R/V *SONNE*

Overall, the three VSLS bromoform, dibromomethane and methyl iodide show a similar pattern of atmospheric mixing ratios (Fig. 6a) along the cruise track with lower atmospheric surface abundances before 21 November 2011, west of Brunei and higher afterwards, which can be attributed to a change in air mass origin as well as an increase of the observed wind speed (Fig. 1). A decrease from 3.4 to 1.2 ppt of bromoform is found at the beginning of the cruise (Fig. 6a) when the ship left Singapore and the coast of the Malaysian Peninsula. On 16–19 November 2011 when the ship passed the southern South China Sea the lower mixing ratios (± standard deviation 1σ) of 1.2 ± 0.3 ppt prevail and also the lowest mixing ratios for bromoform during the whole cruise of 0.8 ppt are found. At the coast of Borneo and the Philippines, the average mixing ratio of bromoform increases to 2.3 ± 1.4 ppt. During the two 24 h stations, the mean mixing ratios are 1.4 ± 0.2 ppt for the first and 2.6 ± 0.4 ppt for the second station. The overall mean bromoform mixing ratio during the cruise is 2.1 ± 1.4 ppt (Table 1) and therefore higher than earlier bromoform observations of 1.2 ppt in January–March 1994 (Yokouchi et al., 1997), 1.1 ppt in September 1994 (Quack and Suess, 1999) and 1.5 ppt in June–July 2009 (Nadzir et al., 2014) further offshore in the South China Sea. The higher atmospheric mixing ratios during the R/V *SONNE* cruise in November 2011 in contrast to the lower mixing ratios in these previous studies may point to stronger local sources, strong seasonal or interannual variations, or even to long-term changes. Dibromomethane shows a mean mixing ratio of 1.2 ± 0.2 ppt (Table 1). Yokouchi et al. (1997) observed a lower mean atmospheric mixing ratio of 0.8 ppt and Nadzir et al. (2014) 1.0 ppt in the South China Sea. An increase of the dibromomethane mixing ratios from 1.0 ± 0.1 ppt to 1.3 ± 0.2 ppt is observed after 21 November 2011 coinciding with an increase of the methyl iodide concentrations from primarily 0.3 ± 0.0 ppt to 0.4 ± 0.1 ppt (Fig. 6a). The highest mixing ratio of methyl iodide was detected in the south western Sulu Sea on 25 November 2011 with 0.8 ppt. The overall mean atmo-

ACPD
15, 17887–17943, 2015

spheric mixing ratio for methyl iodide, of 0.4 ± 0.1 ppt (Table 1) is lower than the mean of 0.6 ppt observed by Yokouchi et al. (1997).

The concentration ratio of dibromomethane and bromoform (Fig. 6b) has been used as an indicator for the age of air masses, after they crossed strong coastal source regions, where a ratio of approximately 0.1 was observed (Yokouchi et al., 2005; Carpenter et al., 2003). The ten times elevated bromoform has a much shorter lifetime, thus degrades more rapidly than dibromomethane, which increases the ratio during transport. Overall, the mean concentration ratio of dibromomethane and bromoform is 0.6 ± 0.2, which suggests that predominantly older air masses are advected over the South China Sea. The highest concentration ratio of 1.2, likely indicating the oldest air mass, is observed on 16 November 2011.

4.2 Oceanic surface concentrations and emissions from R/V *SONNE*

VSLS in the surface sea water along the cruise track show highly variable distributions (Fig. 6c and Table 1). Oceanic bromoform surface concentrations range from 2.8–136.9 pmol L^{-1} with a mean of 19.9 pmol L^{-1} during the cruise, while dibromomethane concentrations range from 2.4–21.8 pmol L^{-1} with a mean of 5.0 pmol L^{-1}. Bromoform and dibromomethane have similar distribution patterns in the sampling region with near shore samples showing typically elevated concentrations. Methyl iodide concentrations range from 0.6–18.8 pmol L^{-1} with a mean of 3.8 pmol L^{-1} and show a different distribution along the ship track than the two bromocarbons, indicating different sources.

High levels of all VSLS are found in waters close to the Malaysian Peninsula, especially in the Singapore Strait on 16 November 2011, likely showing an anthropogenic influence on the VSLS concentrations. VSLS concentrations decrease rapidly when the cruise track leads to open ocean waters. Along the west coast (19–23 November 2011) and north east coast of Borneo (25 November 2011), bromocarbon concentrations are elevated, and especially bromoform concentrations increase in waters influenced by river run.

ACPD
15, 17887–17943, 2015

Oceanic emissions were calculated from synchronized measurements of sea water concentrations and atmospheric mixing ratios, sea surface temperatures and wind speeds, measured on the ship (Sect. 2.3.3). The overall VSLS distribution along the ship track is opposite for the oceanic and atmospheric measurements (Fig. 6a–d). While the sea water concentrations of VSLS generally decrease towards the Sulu Sea, the atmospheric mixing ratios increase, leading to a generally lower concentration gradient of the compounds between sea water and air in the Sulu Sea (not shown here).

Coinciding low VSLS atmospheric background concentrations, high SSTs, elevated oceanic VSLS concentrations and high wind speeds, lead to high emissions of VSLS for the South China and Sulu Sea's (Fig. 6d). In particular, bromoform fluxes are very high and in agreement with coastal fluxes from previous campaigns in tropical source regions (Quack et al., 2007). They often exceed 2000 pmol m^{-2} h^{-1} in the coastal areas and even reach more than 6000 pmol m^{-2} h^{-1} as in the Singapore strait on 15 and on 22 November 2011 at the northwest coast of Borneo, which was also an area of strong convection (Figs. 1, 2, and 6).

4.3 VSLS intercomparison: R/A *FALCON* and R/V *SONNE*

The two profiles of bromocarbon mixing ratios from the surface to 13 km altitude (Sala et al., 2014) and the profile for methyl iodide as observed on R/A *FALCON* with the GhOST and WASP instruments are shown in Fig. 7. Mean bromoform mixing ratios are 1.43 ppt (GhOST) and 1.90 ppt (WASP) in the MABL (0–450 m, determined from meteorological aircraft observations similarly as for the radiosondes, Sect. 2.2.2) and 0.56 ppt (GhOST) and 1.17 ppt (WASP) in the FT (0.45–13 km, Table 1). The GhOST mixing ratios in the MABL are considerably lower than those observed on R/V *SONNE* (2.08 ppt) but higher than the mixing ratios observed by Yokouchi et al. (1997) in January to March 1994, by Quack and Suess (1999) in September 1994 and Nadzir et al. (2014) in June/July 2009 at coastal areas. Open ocean observations of Nadzir et al. (2014) with 1.5 ppt are comparable to GhOST, but lower than WASP observations. A very good agreement of the measurements is given for the longer lived dibromomethane with 1.17 ppt (R/V *SONNE*), 1.19 ppt (GhOST) and 1.15 ppt (WASP). Methyl iodide mixing ratios measured by GhOST are 0.59 ± 0.30 ppt within the MABL of 450 m height, which is about 0.2 ppt higher than the values from R/V *SONNE*, but coincide with the observations by Yokouchi et al. (1997). Above the MABL, the average mixing ratio of methyl iodide decreases to 0.26 ± 0.11 ppt (Fig. 7).

Bromoform and dibromomethane concentrations of all instruments in the MABL correlate with $R = 0.83$ (Fig. 8). Bromoform and methyl iodide concentrations correlate with $R = 0.55$ and dibromomethane and methyl iodide with $R = 0.66$; all three correlations are significant at 99 %. Even higher correlations are found if only measurements on R/V *SONNE* are taken into account with $R = 0.92$ for bromoform and dibromomethane, $R = 0.64$ for bromoform and methyl iodide, and $R = 0.77$ for dibromomethane and methyl iodide.

Two case studies for the comparison of R/A *FALCON* and R/V *SONNE* data are obtained from their meetings on 19 and 21 November 2011 (Table 2), when aircraft and ship passed each other within 100 m distance for several times, measuring the same air masses. During both meetings, deviations between the GhOST and WASP instrument on the aircraft are larger for the bromocarbons than the deviation between the WASP and the ship measurements. WASP and the ship data, which agree very well, rely on sampling of air in stainless steel canisters and subsequent analysis with GC/MS while GhOST measures in situ. Whether this offset is systematic for the different methods, needs to be investigated further. The methyl iodide values of the GhOST and air canister data from the ship show larger differences during the second meeting. In the following, a mean of the GhOST and WASP measurements of R/A *FALCON* is used for computations in the free troposphere.

5 Air mass and VSLS transport from the surface to the free troposphere

5.1 Timescales and intensity of vertical transport

Forward trajectories have been computed with FLEXPART starting at sea level along the cruise track between Singapore to Manila. ERA-Interim is used for the meteorological input (Sect. 2.2.1). The FLEXPART runs yield an average MABL residence time of 7.8 ± 3.5 h before the trajectories enter the FT (Fig. 9), reflecting a relatively fast exchange due to the convective well ventilated MABL (Fig. 5). To estimate the loss of air masses out of the South China Sea area between 5° S–20° N and 100–125° E (Sect. 2.4.3) we determine the loss of trajectories out of this area after their release (Fig. 10). After 4 days 88 % of all trajectories released along the cruise track are still within this defined area of the South China Sea, which decreases to 31 % after 10 days. During these ten days 65.1 ± 22.2 % of the trajectories have passed 6 km height and 20.4 ± 9.7 % have passed 13 km height within the area, while 18.5 % of the trajectories re-enter the MABL from the FT. Most intense convection within FLEXPART calculations along the cruise track occurred on 17 and 18 November 2011 in the southern South China Sea (Fig. 9), 22–24 November at the north western coast of Borneo and on 25–26 November in the Sulu Sea. 30–50 % of the trajectories released from the surface at these times ascend to 13 km height within 3–4 days. Discrepancies to CAPE observations on R/V *SONNE* (Fig. 3) are due to the fact that the calculated CAPE describes the stability of the air column that is observed by the radiosondes ascending with weather balloons, while the trajectories simulate the actual movement of the air masses, thus include the convection in other regions after some hours of transport time. Indeed during convective events at the northern coast of Borneo, the majority of trajectories were transported south towards the coast of Borneo where active convection took part. Trajectories launched between 18–22 November during 00:00 and 12:00 UTC each day reveal a longer residence time of up to 5 days in the lower troposphere (Fig. 9). At about 2 km altitude a barrier seems to suppress convection during this time. This agrees with our CAPE observations, showing suppressed convection at about 1.5 km altitude north

ACPD
15, 17887–17943, 2015

of Borneo (Fig. 3), as lowest observed CAPE is predominantly found between 00:00 and 12:00 UTC during these days.

R/V *SONNE* – R/A *FALCON*: identifying observations of the same air mass

To investigate if the same air masses were observed on R/V *SONNE* and on R/A *FALCON* a perfluorocarbon tracer was released on R/V *SONNE* on 21 November 2011, which was indeed detected 25 h later on R/A *FALCON* (Ren et al., 2015). With the trajectory calculations it can be determined which fraction of the air masses investigated on R/V *SONNE* could subsequently be investigated on R/A *FALCON*. Within a horizontal distance of ±20 km and a maximum vertical distance of ±1 km around the position of the aircraft, as well as a time frame of ±3 h of the VSLS air measurements on R/A *FALCON*, 15 % of all launched 80 × 10 000 surface trajectories, marking the air masses on R/V *SONNE*, passed the R/A *FALCON* flight track during the cruise. Allowing a time frame up to 10 days, the amount of trajectories passing the flight track of R/A *FALCON* increases to 77 ± 29 % between 16 November and 11 December 2011. In the following we combine the R/V *SONNE* and R/A *FALCON* measurements to derive the contribution of oceanic VSLS to MABL and FT concentrations based on the observations.

5.2 Contribution of oceanic emissions to VSLS in the MABL

Computed from observations on R/V *SONNE*, the mean sea–air flux during the cruise is 1486±1718 pmol m^{-2} h^{-1} for bromoform, 405±349 pmol m^{-2} h^{-1} for dibromomethane and 433 ± 482 pmol m^{-2} h^{-1} for methyl iodide (Sect. 4.2). The contribution of the flux to the observed atmospheric VSLS concentration in the MABL (Oceanic Delivery, OD), whose height is determined from the radiosondes, is scaled to 1 day (Table 3, Fig. 11). The OD is 116.4 ± 163.6 % day^{-1} to the MABL concentrations for bromoform, 54.2 ± 66.7 % day^{-1} for dibromomethane and 166.5 ± 185.8 % day^{-1} for methyl iodide. In other words, the oceanic source for bromoform is strong enough to fill up the MABL above the measurement location on average about once per day, while for

ACPD
15, 17887–17943, 2015

dibromomethane the emissions are weaker and nearly 2 days would be required until the observed mixing ratios in the MABL are reached. Based on the FLEXPART trajectories, the mean loss of MABL air to the FT during one day (COnvective Loss, COL) is computed to be $-307.6 \pm 124.3\,\%\,\text{day}^{-1}$. According to the MABL lifetimes of the VSLS the loss due to photolysis and OH, both defined as Chemical Loss (CL) in the MABL is $-6.6\,\%\,\text{day}^{-1}$ for bromoform, $-1.8\,\%\,\text{day}^{-1}$ for dibromomethane and $-30.7\,\%\,\text{day}^{-1}$ for methyl iodide. In order to balance the delivery from the ocean and the loss to the FT and by chemical degradation, an Advective Delivery (AD) of VSLS in and out of the MABL is needed. The AD for bromoform is $197.9 \pm 199.7\,\%\,\text{day}^{-1}$, for dibromomethane $255.2 \pm 131.9\,\%\,\text{day}^{-1}$ and for methyl iodide $171.8 \pm 242.3\,\%\,\text{day}^{-1}$. The numbers indicate that, approximately twice as much VSLS would be advected to reach the MABL mixing ratio, if no OD or COL occurred. OD and AD are transported via COL into the FT. Based on the OD and the COL, the Oceanic Delivery Ratio (ODR) is calculated in order to characterize the relative contribution of the local oceanic emissions compared to the loss of MABL air into the FT (Table 3). The average ODR during the cruise is 0.45 ± 0.55 for bromoform, which means that the loss from the MABL to the FT is balanced to 45 % by oceanic emissions along the cruise track. The ODR for dibromomethane is 0.21 ± 0.21 and for methyl iodide 0.74 ± 1.05, respectively, suggesting that the major amount of methyl iodide origins from nearby sources. Similarly to the ODR the CL is related to the COL to derive the Chemical Loss Ratio (CLR) for the VSLS, which is 0.03 ± 0.01 for bromoform, 0.01 ± 0.00 for dibromomethane and 0.12 ± 0.05 for methyl iodide. When compared to the other source and loss processes, the chemical loss appears negligible for all three gases. The ratio of the advective delivery (ADR) relating the AD to the COL is 0.58 ± 0.55 for bromoform, 0.80 ± 0.21 for dibromomethane and 0.38 ± 1.01, implying that most of the observed dibromomethane (80 %) in the MABL is advected from stronger source regions. Applying the ratios to the observed mixing ratios in the MABL gives an estimate of the amount of the VSLS that origin from local oceanic emissions (VMR_{ODR}) that are degraded chemically (VMR_{CLR}) and that are advected (VMR_{ADR}, Table 4). The local ocean emits a concen-

ACPD
15, 17887–17943, 2015

tration that equates to 0.89 ± 1.12 ppt bromoform, 0.25 ± 0.26 ppt dibromomethane and 0.28 ± 0.40 ppt methyl iodide in the MABL. The amount that is destroyed by chemistry in the MABL before the air is transported into the FT accounts to 0.05 ± 0.04 ppt (bromoform), 0.01 ± 0.01 ppt (dibromomethane) and 0.05 ± 0.03 ppt (methyl iodide). Finally 1.18 ± 1.20 ppt of the observed mixing ratios of bromoform, 0.92 ± 0.27 ppt of dibromomethane and 0.14 ± 0.37 ppt of methyl iodide are advected. The average transport from the MABL to the FT ($Flux_{MABL\text{-}FT}$), computed from the MABL concentrations and the trajectory residence time in the MABL, is 4240 ± 1889 pmol m^{-2} h^{-1} for bromoform, 2419 ± 929 pmol m^{-2} h^{-1} for dibromomethane and 865 ± 373 pmol m^{-2} h^{-1} for methyl iodide. Calculations with the ERA-Interim MABL height, which is on average 140 m higher than the radiosonde derived one, leads to very similar estimates (Appendix 1).

Since the wind is a driving factor for oceanic emissions and advection of VSLS, changes in wind speed are assumed to affect atmospheric VSLS mixing ratios in the MABL during this cruise. Significant correlations are found between wind speed and the observed mixing ratios of all three VSLS in the MABL with correlation coefficients of $R = 0.55$ (bromoform), $R = 0.57$ (dibromomethane) and $R = 0.56$ (methyl iodide), respectively. The according amount of mixing ratios that origin from the oceanic emissions (VMR_{ODR}) correlate significantly to the wind speed with $R = 0.52$, $R = 0.72$ and $R = 0.62$, respectively. On the opposite, VMR_{ADR}, which is calculated as the residual from VMR_{ODR}, is negative correlated to the wind speed with $R = -0.21$, $R = -0.32$ and $R = -0.53$. The correlations reveal that the contribution of oceanic emissions to MABL VSLS increase for higher wind speeds, while the advective contribution decreases.

5.3 Oceanic contribution to the FT

5.3.1 Identification of MABL air and their contained VSLS in the FT

With a simplified approach (method description in Sect. 2.4.3) we are able to estimate the contribution of MABL air and regional marine sources observed on R/V *SONNE* to the FT. Individual MABL air masses during the cruise contribute on average over 20 %

ACPD
15, 17887–17943, 2015

to the lowest FT air right after they leave 0.5 km altitude (Fig. 12). Within 2–6 days after crossing that level an observed MABL air mass contributes up to 15 % depending on the height. A decrease of the contribution with height down to 3 % occurs until 8 km altitude. Above this height, the contribution of the MABL air masses increases again to over 5 % as a result of the density driven extension of the air parcels. The temporal decrease due to the transport of trajectories out of the predefined South China and Sulu Seas area (Fig. 10) is visible after three days.

The average contribution of VSLS from the MABL air to the FT mixing ratio (c_{MABL}) between 2 and 11 km altitude within 10 days after release is with 1–28 % highest for bromoform followed by 1–12 % for dibromomethane and only 0–5 % for the short-lived methyl iodide (coloured contours in Fig. 12). For all compounds, the largest contributions of > 25 % are found between 0.5 and 2 km height within the first 2 days after release due to occasional fresh entrainment of MABL air. Above 8 km altitude, the average contribution of the individual MABL VSLS releases increase again to > 11 % (bromoform), > 5 % (dibromomethane) and > 3 % (methyl iodide), due to the density driven extension of the MABL air parcels with height. The chemical degradation of methyl iodide, according to its short tropospheric lifetime of 4 days is visible already 2 days after release, when its contribution decreases to < 7 % within 0.5–2.5 km altitude and to < 2.5 % above 2.5 km altitude. To identify the contribution of the oceanic emissions to the FT VSLS during the cruise, the $\mathrm{VMR_{ODR}}$ of each compound is used as the initial mixing ratio in the MABL air mass. The mean contribution of marine compounds from the South China Sea to the FT air varies with time and altitude, but is generally higher for bromoform with 1–13 % than for methyl iodide with 0–4 %. This is not surprising, considering the longer lifetime of bromoform compared to methyl iodide, although the relative contribution of oceanic emissions to MABL air (Sect. 5.2) was identified to be higher for methyl iodide (74 %) than for bromoform (45 %). The low mean regional marine contribution of dibromomethane to the observed MABL mixing ratio of 21 % is also reflected in its mean oceanic contribution of only 0–3 % to the FT air masses.

ACPD
15, 17887–17943, 2015

5.3.2 Accumulated VSLS in the free troposphere

By simulating a steady transport of MABL air masses into the FT, mean accumulated VSLS mixing ratios in the FT along and during the cruise were computed (Fig. 13) as described in 2.4.3. The simulated FT mixing ratios of bromoform and dibromomethane from the observed MABL (VMR_{MABL}) decrease on average from 1.8 and 1.1 ppt at 0.5 km height to 0.7 ppt respectively 0.6 ppt at 7 km height and increase again above 8 km up to 0.9 ppt (bromoform) and 0.8 ppt (dibromomethane). Simulated methyl iodide shows a decrease from 0.21 ppt at 0.5 km to 0.06 ppt at 3 km. Above this altitude, the simulated mixing ratios of methyl iodide are quite constant 0.06 ppt.

To estimate the accumulated FT mixing ratios solely from oceanic emissions, the VMR_{ODR} is used as the initial MABL mixing ratio (Fig. 13). The simulated FT mixing ratios using either VMR_{MABL} or VMR_{ODR} as input reveal a similar vertical pattern, since both simulations are based on the same meteorology and trajectories. While FT mixing ratios based on VMR_{MABL} and VMR_{ODR} are similar for methyl iodide (due to the large oceanic contribution to the MABL mixing ratios), FT mixing ratios from VMR_{ODR} are on average ~ 0.5 ppt lower for bromoform and ~ 0.6 ppt dibromomethane than from VMR_{MABL}. Comparing the simulated VMR_{MABL} FT mixing ratios with the observed FT mixing ratios from R/A *FALCON* reveals stronger vertical variations for the simulations in contrast to the observations. Bromoform is overestimated in the VMR_{MABL} simulation between 0.5 and 7 km altitude, as well as between 9 and 12 km. Simulated dibromomethane in the FT based on VMR_{MABL} underestimates the observed mixing ratios between 3 and 12 km height. In particular, the maximum between 6 and 9 km height is not reflected in the simulations. However, observations of both bromocarbons are within 1σ of the FT simulations with MABL air. The methyl iodide simulations show a distinct underestimation of the observed FT mixing ratios. In Sect. 4.3 we have shown that methyl iodide measured in same air masses by R/V *SONNE* and R/A *FALCON* was 51 % higher for the aircraft (Table 2). Adjusting all R/A *FALCON* values by this identi-

Discussion Paper | Discussion Paper | Discussion Paper | Discussion Paper |

ACPD

15, 17887–17943, 2015

The contribution of oceanic halocarbons to marine and free troposphere air

S. Fuhlbrügge et al.

fied offset to R/V *SONNE* reveals a better agreement between observed and simulated FT mixing ratios (Fig. 13).

5.3.3 Discussion

The simulations show how local oceanic emissions and advection of remote air can explain the observed FT mixing ratios (Fig. 13). Local oceanic emissions of bromoform from the South China Sea contribute about 60 % to the FT mixing ratios. However, simulations based on the MABL mixing ratios clearly overestimate the observations in the FT. In order to explain the FT bromoform profiles from the aircraft observations, we need to take into account advection from other FT regions within the South China Sea. This FT advection leads to lower bromoform than the convection out of the MABL along the cruise track. The bromoform found in the MABL originates to 45 % from local sources along the ship track. Accordingly, advection from strong source regions, possibly along the coast, is necessary to explain the remaining 55 % of the bromoform abundance. The fact that the MABL bromoform observed along the cruise track is too high for the local emissions and also too high for the FT profiles above the South China Sea, suggests that the local MABL observations are impacted by additional stronger source regions and may not be representative for the whole region. Observations of lower atmospheric bromoform mixing ratios by Yokouchi et al. (1997), Quack and Suess (1999) and Nadzir et al. (2014) in the South China Sea (Sect. 4.1) confirm this assumption.

Dibromomethane in the FT derived from MABL abundances matches the aircraft observations quite well, indicating that dibromomethane observations in the MABL along the cruise track are representative for the region. While in the FT, advection of air masses with different mixing ratios is not necessary to explain the observed dibromomethane, the situation is reversed in the MABL. Significant advection of dibromomethane-rich air is necessary to explain the observations in the MABL, since only low oceanic sources were observed during the cruise. The impact of advection on the dibromomethane mixing ratio is enhanced by its relatively long tropospheric lifetime of 120 days.

ACPD
15, 17887–17943, 2015

In contrast to bromoform and dibromomethane, the simulated mixing ratios of methyl iodide in the FT are strongly underestimated no matter whether observed MABL mixing ratios or oceanic emissions are used. Due to its short tropospheric life time of 4 days methyl iodide is rapidly degraded during the transport into the FT. The offset between the simulated and observed FT methyl iodide could be caused by additional strong sources of methyl iodide in the South China Sea area. Furthermore, modelling or measurement uncertainties may add to this offset, which we all discuss in the following:

The simulations use constant atmospheric lifetimes for each compound and neglect variations with altitude which could impact the simulated abundances. However, the altitude variations of methyl iodide in the MABL and FT are around 0.5 days (WMO, 2015) and thus are quite small. Therefore it seems unlikely that the lifetime estimate causes a large underestimation of the FT methyl iodide. Deficiencies in the meteorological input fields and the FLEXPART model, in particular in the boundary layer and in the convection parameterizations would affect all compounds and their contribution to the FT concentrations in a similar way and thus seems to be unlikely as well. Ship and aircraft measurements reveal instrumental offsets, while observing the same air masses, which cannot be resolved due to the different applied calibration scales (Sect. 4.3). When we adjust for a constant factor, by which observations of methyl iodide in the MABL differed between R/V *SONNE* and R/A *FALCON*, the simulated and observed FT mixing ratios match better. Thus, an instrumental offset causing, at least partially, the calculated discrepancy for methyl iodide appears likely (Sect. 2.3.1).

Another explanation for the elevated methyl iodide in the FT is advection of fresh air with elevated methyl iodide mixing ratio in the FT from e.g. South East Asia or the Philippines. These areas are known to comprise strong sources for atmospheric methyl iodide from e.g. rice plantation (Redeker et al., 2003; Lee-Taylor and Redeker, 2005). In combination with convective activity over land, which is common in this area (Hendon and Woodberry, 1993), the high observed FT mixing ratios of methyl iodide could be explained, despite the low oceanic contribution during the cruise. The low observed MABL mixing ratios of methyl iodide on R/V *SONNE* may thus also not be represen-

ACPD
15, 17887–17943, 2015

tative for the area. Yokouchi et al. (1997) observed higher atmospheric methyl iodide mixing ratios in the South China Sea. Finally, the method of our simplified approach includes uncertainties as well. Since observational studies quantifying the oceanic contribution to atmospheric abundances of VSLS are quite rare, it is difficult to evaluate our findings at the moment and more studies for different oceanic regimes should be carried out to validate our results.

6 Summary

The contribution of oceanic VSLS emissions to marine atmospheric boundary layer (MABL) and free troposphere (FT) air during the SHIVA campaign in November 2011 in the South China and Sulu Seas was investigated in this study. Meteorological parameters were measured near the ocean surface and in the troposphere by regular radiosonde launches on R/V *SONNE* during the cruise. Oceanic VSLS emissions were determined from atmospheric and sea surface water concentration observations. The transport from the surface through the MABL into the FT was computed with the trajectory model FLEXPART.

The ship cruise was dominated by north-easterly winds with a characteristic moderate mean wind speed of 5.5 $m\,s^{-1}$. The radiosonde launches revealed the high convective potential of the South China and Sulu Seas with an average convective available potential energy (CAPE) of $998 \pm 629\,J\,kg^{-1}$ and a convective, well ventilated, weakly developed MABL with an average height of 420 ± 120 m during the cruise. 800 000 forward trajectories, launched from the ocean surface along the cruise track, show a rapid exchange of MABL air with the FT within 7.8 h. This study concentrates on the three very short lived substances bromoform, dibromomethane and methyl iodide which are known to impact tropospheric and stratospheric ozone. On the one hand, the observations on R/V *SONNE* reveal high mean ocean surface concentrations and emissions for bromoform (19.94 $pmol\,L^{-1}$ and 1486 $pmol\,m^{-2}\,h^{-1}$), dibromomethane (4.99 $pmol\,L^{-1}$ and 405 $pmol\,m^{-2}\,h^{-1}$) and methyl iodide (3.82 $pmol\,L^{-1}$ and 433 $pmol\,m^{-2}\,h^{-1}$) in comparison to other oceanic source regions. Atmospheric mixing ratios in the MABL, on the other hand, are relatively low compared to earlier campaigns with mean values of 2.08 ppt bromoform, 1.17 ppt dibromomethane, and 0.39 ppt methyl iodide. The contribution of the oceanic VSLS emissions to their MABL concentrations was evaluated by simple source-loss estimations, resulting in an Oceanic Delivery Ratio (ODR). The ODR for bromoform is computed to be 0.45, revealing that bromoform mixing ratios in the MABL above the marginal seas originated on average to 45 % from local oceanic sources. The ODR for dibromomethane is 21 % and for methyl iodide 74 % indicating that the long-lived dibromomethane is largely advected in the MABL, while the short-lived methyl iodide originates mainly from the local ocean.

We extend our analysis to the FT using VSLS profiles obtained from observations on the research aircraft (R/A) *FALCON* above the South China Sea. The average contribution of a single MABL air release to the FT mixing ratios (Sect. 5.3.1) is up to 28 % (bromoform), 12 % (dibromomethane) and 5 % (methyl iodide). The mean contributions of the local oceanic VSLS to the FT within this MABL air release are up to 13 % (bromoform), 3 % (dibromomethane) and 4 % (methyl iodide). In order to estimate if the accumulated contribution from the single MABL air releases is sufficient to explain the accumulated VSLS mixing ratios observed in the FT, we simulate a steady transport of observed MABL air masses, respectively, oceanic emissions into the FT above the South China Sea. The simulations for bromoform based on the volume mixing ratios in the MABL (VMR_{MABL}) overestimated the observations in the FT, while the simulations based on the local oceanic emissions of bromoform from the South China Sea (VMR_{ODR}) explained about 60 % of the observed FT mixing ratio. In the MABL the local oceanic emissions along the cruise track can also explain half of the bromoform which is also too high for the FT observations. Thus, we conclude that the observed mixing ratios of bromoform in the MABL are influenced by stronger local sources and may not be representative for the whole South China Sea where we expect generally lower values.

ACPD
15, 17887–17943, 2015

Title Page
Abstract | Introduction
Conclusions | References
Tables | Figures
|◀ | ▶|
◀ | ▶
Back | Close
Full Screen / Esc
Printer-friendly Version
Interactive Discussion

Dibromomethane in the FT, simulated from observed MABL mixing ratios, shows a good agreement between observations and simulations. It is most likely mixed in the FT with advected air masses containing similar dibromomethane mixing ratios. Methyl iodide in the FT is strongly underestimated in the simulations, using both the observed MABL mixing ratios and the oceanic emissions. The disagreement points either to an unresolved offset between the ship and aircraft data, or to an underestimation of representative methyl iodide MABL mixing ratios and to additional methyl iodide sources, e.g. rice plantations in South East Asia that were not covered by the ship cruise.

Our investigations show how oceanic emissions of VSLS in a strong oceanic source region contribute to the observed atmospheric mixing ratios in the MABL. Furthermore, the contributions of these atmospheric mixing ratios and the local oceanic VSLS therein to the VSLS, observed in the FT above this source region, are derived. The results reveal strong links between oceanic emissions, atmospheric mixing ratios, MABL conditions and prevailing convective activity in the troposphere. The methods should be applied to other oceanic regions to derive a better process understanding of the contributions of air–sea gas exchange on atmospheric abundances. For the detection of future climate change effects on ocean surface trace gas emissions and their influence on atmospheric chemistry and composition it is important to study the complex interplay between oceanic sources and emissions, meteorology, atmospheric mixing ratios, and transport to the upper atmosphere.

Acknowledgements. This work was supported by the EU project SHIVA under grant agreement no. FP7-ENV-2007-1-226224 and by the BMBF grants SHIVA-SONNE 03G0218A and SOPRAN II FKZ 03F0611A. We thank the authorities of Malaysia and the Philippines for the permissions to work in their territorial waters, as well as the SHIVA coordinators Klaus Pfeilsticker and Marcel Dorf and all other SHIVA contributors. We acknowledge the European Centre for medium range weather forecast (ECMWF) for the provision of ERA-Interim reanalysis data and the Lagrangian particle dispersion model FLEXPART used in this publication. We would also like to thank for the support, the captain and crew of R/V *SONNE* and the pilot in command and crew of R/A *FALCON* as well as the Projektträger Jülich (PTJ) and the Deutscher Wetterdienst (DWD). E. Atlas was supported by grant #NNX12AH02G from the NASA Upper

Atmosphere Research Program. We thank X. Zhu and L. Pope for technical support of canister analysis.

References

Aschmann, J. and Sinnhuber, B.-M.: Contribution of very short-lived substances to stratospheric bromine loading: uncertainties and constraints, Atmos. Chem. Phys., 13, 1203–1219, doi:10.5194/acp-13-1203-2013, 2013.

Aschmann, J., Sinnhuber, B.-M., Chipperfield, M. P., and Hossaini, R.: Impact of deep convection and dehydration on bromine loading in the upper troposphere and lower stratosphere, Atmos. Chem. Phys., 11, 2671–2687, doi:10.5194/acp-11-2671-2011, 2011.

Brinckmann, S., Engel, A., Bönisch, H., Quack, B., and Atlas, E.: Short-lived brominated hydrocarbons – observations in the source regions and the tropical tropopause layer, Atmos. Chem. Phys., 12, 1213–1228, doi:10.5194/acp-12-1213-2012, 2012.

Carpenter, L. and Liss, P.: On temperate sources of bromoform and other reactive organic bromine gases, J. Geophys. Res.-Atmos., 105, 20539–20547, doi:10.1029/2000JD900242, 2000.

Carpenter, L., Liss, P., and Penkett, S.: Marine organohalogens in the atmosphere over the Atlantic and Southern Oceans, J. Geophys. Res.-Atmos., 108, 4256, doi:10.1029/2002JD002769, 2003.

Carpenter, L. J., Reimann, S., Burkholder, J. B., Clerbaux, C., Hall, B. D., Hossaini, R., Laube, J. C., and Yvon-Lewis, S. A.: Update on Ozone-Depleting Substances (ODSs) and other gases of interest to the Montreal Protocol, in: Scientific Assessment of Ozone Depletion: 2014, edited by: Engel, A. and Montzka, S. A., World Meteorological Organization, Geneva, 2014.

Dee, D., Uppala, S., Simmons, A., Berrisford, P., Poli, P., Kobayashi, S., Andrae, U., Balmaseda, M., Balsamo, G., Bauer, P., Bechtold, P., Beljaars, A., van de Berg, L., Bidlot, J., Bormann, N., Delsol, C., Dragani, R., Fuentes, M., Geer, A., Haimberger, L., Healy, S., Hersbach, H., Holm, E., Isaksen, L., Kallberg, P., Kohler, M., Matricardi, M., McNally, A., Monge-Sanz, B., Morcrette, J., Park, B., Peubey, C., de Rosnay, P., Tavolato, C., Thepaut, J., and Vitart, F.: The ERA-Interim reanalysis: configuration and performance of the data assimilation system, Q. J. Roy. Meteor. Soc., 137, 553–597, doi:10.1002/qj.828, 2011.

Dix, B., Baidara, S., Bresch, J., Hall, S., Schmidt, K., Wang, S., and Volkamer, R.: Detection of iodine monoxide in the tropical free troposphere, P. Natl. Acad. Sci. USA, 110, 2035–2040, doi:10.1073/pnas.1212386110, 2013.

Forster, C., Stohl, A., and Seibert, P.: Parameterization of convective transport in a Lagrangian particle dispersion model and its evaluation, J. Appl. Meteorol. Clim., 46, 403–422, doi:10.1175/JAM2470.1, 2007.

Fuhlbrügge, S., Krüger, K., Quack, B., Atlas, E., Hepach, H., and Ziska, F.: Impact of the marine atmospheric boundary layer conditions on VSLS abundances in the eastern tropical and subtropical North Atlantic Ocean, Atmos. Chem. Phys., 13, 6345–6357, doi:10.5194/acp-13-6345-2013, 2013.

Gschwend, P., Macfarlane, J., and Newman, K.: Volatile halogenated organic-compounds released to seawater from temperate marine macroalgae, Science, 227, 1033–1035, doi:10.1126/science.227.4690.1033, 1985.

Hendon, H. and Woodberry, K.: The diurnal cycle of tropical convection, J. Geophys. Res.-Atmos., 98, 16623–16637, doi:10.1029/93JD00525, 1993.

Hepach, H., Quack, B., Ziska, F., Fuhlbrügge, S., Atlas, E. L., Krüger, K., Peeken, I., and Wallace, D. W. R.: Drivers of diel and regional variations of halocarbon emissions from the tropical North East Atlantic, Atmos. Chem. Phys., 14, 1255–1275, doi:10.5194/acp-14-1255-2014, 2014.

Hossaini, R., Chipperfield, M. P., Monge-Sanz, B. M., Richards, N. A. D., Atlas, E., and Blake, D. R.: Bromoform and dibromomethane in the tropics: a 3-D model study of chemistry and transport, Atmos. Chem. Phys., 10, 719–735, doi:10.5194/acp-10-719-2010, 2010.

Hossaini, R., Mantle, H., Chipperfield, M. P., Montzka, S. A., Hamer, P., Ziska, F., Quack, B., Krüger, K., Tegtmeier, S., Atlas, E., Sala, S., Engel, A., Bönisch, H., Keber, T., Oram, D., Mills, G., Ordóñez, C., Saiz-Lopez, A., Warwick, N., Liang, Q., Feng, W., Moore, F., Miller, B. R., Marécal, V., Richards, N. A. D., Dorf, M., and Pfeilsticker, K.: Evaluating global emission inventories of biogenic bromocarbons, Atmos. Chem. Phys., 13, 11819–11838, doi:10.5194/acp-13-11819-2013, 2013.

Ko, M. K. W., Poulet, G., and Blake, D. R.: Very Short-Lived Halogen and Sulfur Substances, Scientific Assessment of Ozone Depletion: 2002, Global Ozone Research and Monitoring Project, Chapter 2, report No. 47, World Meteorological Organization, Geneva, 2003.

ACPD
15, 17887–17943, 2015

Krüger, K. and Quack, B.: Introduction to special issue: the *TransBrom Sonne* expedition in the tropical West Pacific, Atmos. Chem. Phys., 13, 9439–9446, doi:10.5194/acp-13-9439-2013, 2013.
Lee-Taylor, J. and Redeker, K.: Reevaluation of global emissions from rice paddies of methyl iodide and other species, Geophys. Res. Lett., 32, L15801, doi:10.1029/2005GL022918, 2005.
Liu, Y., Yvon-Lewis, S., Thornton, D., Butler, J., Bianchi, T., Campbell, L., Hu, L., and Smith, R.: Spatial and temporal distributions of bromoform and dibromomethane in the Atlantic Ocean and their relationship with photosynthetic biomass, J. Geophys. Res.-Oceans, 118, 3950–3965, doi:10.1002/jgrc.20299, 2013.
Margules, M.: Über die Energie der Stürme, K. K. Zentralanstalt für Meteorologie und Erdmagnetismus in Wien, Vienna, 1–26, 1905.
Moncrieff, M. and Miller, M.: Dynamics and simulation of tropical cumulonimbus and squall lines, Q. J. Roy. Meteor. Soc., 102, 373–394, doi:10.1002/qj.49710243208, 1976.
Montzka, S., Butler, J., Hall, B., Mondeel, D., and Elkins, J.: A decline in tropospheric organic bromine, Geophys. Res. Lett., 30, 1826, doi:10.1029/2003GL017745, 2003.
Montzka, S. A. and Reimann, S.: Ozone-depleting substances and related chemicals, Scientific Assessment of Ozone Depletion: 2010, Global Ozone Research and Monitoring Project – Report No. 52, Geneva, Switzerland, 2011.
Mohd Nadzir, M. S., Phang, S. M., Abas, M. R., Abdul Rahman, N., Abu Samah, A., Sturges, W. T., Oram, D. E., Mills, G. P., Leedham, E. C., Pyle, J. A., Harris, N. R. P., Robinson, A. D., Ashfold, M. J., Mead, M. I., Latif, M. T., Khan, M. F., Amiruddin, A. M., Banan, N., and Hanafiah, M. M.: Bromocarbons in the tropical coastal and open ocean atmosphere during the 2009 Prime Expedition Scientific Cruise (PESC-09), Atmos. Chem. Phys., 14, 8137–8148, doi:10.5194/acp-14-8137-2014, 2014.
Nightingale, P., Malin, G., Law, C., Watson, A., Liss, P., Liddicoat, M., Boutin, J., and Upstill-Goddard, R.: In situ evaluation of air–sea gas exchange parameterizations using novel conservative and volatile tracers, Global Biogeochem. Cy., 14, 373–387, doi:10.1029/1999GB900091, 2000.
Quack, B. and Suess, E.: Volatile halogenated hydrocarbons over the western Pacific between 43 and 4° N, J. Geophys. Res.-Atmos., 104, 1663–1678, doi:10.1029/98JD02730, 1999.
Quack, B. and Wallace, D.: Air–sea flux of bromoform: controls, rates, and implications, Global Biogeochem. Cy., 17, 1023, doi:10.1029/2002GB001890, 2003.

ACPD
15, 17887–17943, 2015

Quack, B., Atlas, E., Petrick, G., and Wallace, D.: Bromoform and dibromomethane above the Mauritanian upwelling: atmospheric distributions and oceanic emissions, J. Geophys. Res.-Atmos., 112, D09312, doi:10.1029/2006JD007614, 2007.

Quack, B., Krüger, K., Atlas, E., Tegtmeier, S., Großmann, K., Rex, M., von Glasow, R., Sommariva, R., and Wallace, D.: Halocarbon sources and emissions over the Western Pacific, oral presentation, EGU General Assembly, 5 April 2011, Vienna, Austria, 2011.

Redeker, K., Meinardi, S., Blake, D., and Sass, R.: Gaseous emissions from flooded rice paddy agriculture, J. Geophys. Res.-Atmos., 108, 4386, doi:10.1029/2002JD002814, 2003.

Ren, Y., Baumann, R., and Schlager, H.: An airborne perfluorocarbon tracer system and its first application for a Lagrangian experiment, Atmos. Meas. Tech., 8, 69–80, doi:10.5194/amt-8-69-2015, 2015.

Saiz-Lopez, A. and von Glasow, R.: Reactive halogen chemistry in the troposphere, Chem. Soc. Rev., 41, 6448–6472, doi:10.1039/c2cs35208g, 2012.

Sala, S., Bönisch, H., Keber, T., Oram, D. E., Mills, G., and Engel, A.: Deriving an atmospheric budget of total organic bromine using airborne in situ measurements from the western Pacific area during SHIVA, Atmos. Chem. Phys., 14, 6903–6923, doi:10.5194/acp-14-6903-2014, 2014.

Schauffler, S., Atlas, E., Blake, D., Flocke, F., Lueb, R., Lee-Taylor, J., Stroud, V., and Travnicek, W.: Distributions of brominated organic compounds in the troposphere and lower stratosphere, J. Geophys. Res.-Atmos., 104, 21513–21535, doi:10.1029/1999JD900197, 1999.

Seibert, P., Beyrich, F., Gryning, S., Joffre, S., Rasmussen, A., and Tercier, P.: Review and intercomparison of operational methods for the determination of the mixing height, Atmos. Environ., 34, 1001–1027, doi:10.1016/S1352-2310(99)00349-0, 2000.

Solomon, S.: Stratospheric ozone depletion: a review of concepts and history, Rev. Geophys., 37, 275–316, doi:10.1029/1999RG900008, 1999.

Solomon, S., Garcia, R., and Ravishankara, A.: On the role of iodine in ozone depletion, J. Geophys. Res.-Atmos., 99, 20491–20499, doi:10.1029/94JD02028, 1994.

Sorensen, J.: Sensitivity of the DERMA long-range gaussian dispersion model to meteorological input and diffusion parameters, Atmos. Environ., 32, 4195–4206, doi:10.1016/S1352-2310(98)00178-2, 1998.

Stohl, A. and Thomson, D.: A density correction for Lagrangian particle dispersion models, Bound.-Lay. Meteorol., 90, 155–167, doi:10.1023/A:1001741110696, 1999.

ACPD
15, 17887–17943, 2015

Stohl, A. and Trickl, T.: A textbook example of long-range transport: Simultaneous observation of ozone maxima of stratospheric and North American origin in the free troposphere over Europe, J. Geophys. Res.-Atmos., 104, 30445–30462, doi:10.1029/1999JD900803, 1999.
Stohl, A., Hittenberger, M., and Wotawa, G.: Validation of the Lagrangian particle dispersion model FLEXPART against large-scale tracer experiment data, Atmos. Environ., 32, 4245–4264, doi:10.1016/S1352-2310(98)00184-8, 1998.
Stohl, A., Forster, C., Frank, A., Seibert, P., and Wotawa, G.: Technical note: The Lagrangian particle dispersion model FLEXPART version 6.2, Atmos. Chem. Phys., 5, 2461–2474, doi:10.5194/acp-5-2461-2005, 2005.
Stull, R.: An Introduction to Boundary Layer Meteorology, Kluwer Academic Publishers, Dordrecht, 1988.
Tegtmeier, S., Krüger, K., Quack, B., Atlas, E. L., Pisso, I., Stohl, A., and Yang, X.: Emission and transport of bromocarbons: from the West Pacific ocean into the stratosphere, Atmos. Chem. Phys., 12, 10633–10648, doi:10.5194/acp-12-10633-2012, 2012.
Tegtmeier, S., Krüger, K., Quack, B., Atlas, E., Blake, D. R., Boenisch, H., Engel, A., Hepach, H., Hossaini, R., Navarro, M. A., Raimund, S., Sala, S., Shi, Q., and Ziska, F.: The contribution of oceanic methyl iodide to stratospheric iodine, Atmos. Chem. Phys., 13, 11869–11886, doi:10.5194/acp-13-11869-2013, 2013.
Thompson, R. and Edwards, R.: An overview of environmental conditions and forecast implications of the 3 May 1999 tornado outbreak, Weather Forecast., 15, 682–699, doi:10.1175/1520-0434(2000)015<0682:AOOECA>2.0.CO;2, 2000.
Troen, I. and Mahrt, L.: A simple-model of the atmospheric boundary-layer: Sensitivity to surface evaporation, Bound.-Lay. Meteorol., 37, 129–148, doi:10.1007/BF00122760, 1986.
Vogelezang, D. and Holtslag, A.: Evaluation and model impacts of alternative boundary-layer height formulations, Bound.-Lay. Meteorol., 81, 245–269, doi:10.1007/BF02430331, 1996.
von Glasow, R., von Kuhlmann, R., Lawrence, M. G., Platt, U., and Crutzen, P. J.: Impact of reactive bromine chemistry in the troposphere, Atmos. Chem. Phys., 4, 2481–2497, doi:10.5194/acp-4-2481-2004, 2004.
WMO: Scientific Assessment of Ozone Depletion: 2014, Global Ozone Research and Monitoring Project, Geneva, Switzerland, 2015.
Worton, D., Mills, G., Oram, D., and Sturges, W.: Gas chromatography negative ion chemical ionization mass spectrometry: application to the detection of alkyl nitrates and halocarbons

ACPD
15, 17887–17943, 2015

in the atmosphere, J. Chromatogr. A, 1201, 112–119, doi:10.1016/j.chroma.2008.06.019, 2008.
Yang, X., Cox, R., Warwick, N., Pyle, J., Carver, G., O'Connor, F., and Savage, N.: Tropospheric bromine chemistry and its impacts on ozone: a model study, J. Geophys. Res.-Atmos., 110, D23311, doi:10.1029/2005JD006244, 2005.
Yang, X., Abraham, N. L., Archibald, A. T., Braesicke, P., Keeble, J., Telford, P. J., Warwick, N. J., and Pyle, J. A.: How sensitive is the recovery of stratospheric ozone to changes in concentrations of very short-lived bromocarbons?, Atmos. Chem. Phys., 14, 10431–10438, doi:10.5194/acp-14-10431-2014, 2014.
Yokouchi, Y., Mukai, H., Yamamoto, H., Otsuki, A., Saitoh, C., and Nojiri, Y.: Distribution of methyl iodide, ethyl iodide, bromoform, and dibromomethane over the ocean (east and southeast Asian seas and the western Pacific), J. Geophys. Res.-Atmos., 102, 8805–8809, doi:10.1029/96JD03384, 1997.
Yokouchi, Y., Hasebe, F., Fujiwara, M., Takashima, H., Shiotani, M., Nishi, N., Kanaya, Y., Hashimoto, S., Fraser, P., Toom-Sauntry, D., Mukai, H., and Nojiri, Y.: Correlations and emission ratios among bromoform, dibromochloromethane, and dibromomethane in the atmosphere, J. Geophys. Res.-Atmos., 110, D23309, doi:10.1029/2005JD006303, 2005.

ACPD
15, 17887–17943, 2015

Table 1. Mean ± standard deviation and range ([ ]) of atmospheric mixing ratios observed on R/V *SONNE* and R/A *FALCON* (GhOST-MS and WASP GC/MS) in the MABL and the FT, water concentrations observed by R/V *SONNE* and computed the sea–air flux. MABL and FT mixing ratios for bromoform and dibromomethane on R/A *FALCON* are adopted from Sala et al. (2014). The R/A *FALCON* MABL height was set to 450 m. The last line gives the sea–air flux computed from R/V *SONNE* mixing ratios for all three compounds.

				Bromoform	Dibromomethane	Methyl iodide
Atmosph. mixing ratios [ppt]	R/V *SONNE*			2.08 ± 1.36 [0.79–5.07]	1.17 ± 0.19 [0.71–1.98]	0.39 ± 0.09 [0.19–0.78]
	R/A *FALCON*	GhOST	MABL	1.43 ± 0.53 [0.42–3.42]	1.19 ± 0.21 [0.58–1.89]	0. 59 ± 0.30 [0.29–3.23]
			FT	0.56 ± 0.17 [0.16–2.15]	0.87 ± 0.12 [0.56–1.54]	0.26 ± 0.11 [0.08–0.80]
		WASP	MABL	1.90 ± 0.55 [0.99–3.78]	1.15 ± 0.14 [0.85–1.59]	/
			FT	1.17 ± 0.50 [0.43–3.22]	0.88 ± 0.14 [0.46–1.36]	/
Water concentrations [pmol L^{-1}]				19.94 ± 17.90 [2.80–136.91]	4.99 ± 2.59 [2.43–21.82]	3.82 ± 2.43 [0.55–18.84]
Sea–air flux [pmol m^{-2} h^{-1}]				1486 ± 1718 [−8–13 149]	405 ± 349 [16–2210]	433 ± 482 [13–2980]

ACPD
15, 17887–17943, 2015

Table 2. Mean atmospheric mixing ratios of bromoform, dibromomethane and methyl iodide observed on R/V *SONNE* and R/A *FALCON* during two case studies on 19 November 2011 at 3.2° N and 112.5° E and on 21 November 2011 at 4.6° N and 113.0° E.

		Bromoform [ppt]	Dibromomethane [ppt]	Methyl iodide [ppt]
19 Nov 2011	R/V *SONNE*	1.37	0.99	0.29
	R/A *FALCON*: GhOST/WASP	1.02/1.37	0.94/1.03	0.45/–
21 Nov 2011	R/V *SONNE*	2.05	1.08	0.28
	R/A *FALCON*: GhOST/WASP	1.63/2.00	1.31/1.08	0.82/–

ACPD
15, 17887–17943, 2015

Table 3. Mean ± standard deviation of Oceanic Delivery (OD), COnvective Loss (COL), Chemical Loss (CL), Advective Delivery (AD), Oceanic Delivery Ratio (ODR), Chemical Loss Ratio (CLR), Advective Delivery Ratio (ADR) for bromoform ($CHBr_3$), dibromomethane (CH_2Br_2) and methyl iodide (CH_3I).

	OD [% day^{-1}]	COL [% day^{-1}]	CL [% day^{-1}]	AD [% day^{-1}]	ODR	CLR	ADR
$CHBr_3$	116.4 ± 163.6	−307.6 ± 124.3	−6.6	197.9 ± 199.7	0.45 ± 0.55	−0.03 ± 0.01	0.58 ± 0.55
CH_2Br_2	54.2 ± 66.7	−307.6 ± 124.3	−1.8	255.2 ± 131.9	0.21 ± 0.21	−0.01 ± 0.00	0.80 ± 0.21
CH_3I	166.5 ± 185.8	−307.6 ± 124.3	−30.7	171.8 ± 242.3	0.74 ± 1.05	−0.12 ± 0.05	0.38 ± 1.01

ACPD
15, 17887–17943, 2015

Table 4. Mean ± standard deviation of observed Volume Mixing Ratios in the MABL on R/V *SONNE* (VMR_{MABL}) vs. the amount of VMR originating from oceanic emissions (VMR_{ODR}), chemically degraded according to the specific lifetime (VMR_{CLR}), originating from advection (VMR_{ADR}) and the Flux from the MABL into the FT ($Flux_{MABL\text{-}FT}$) for bromoform ($CHBr_3$), dibromomethane (CH_2Br_2) and methyl iodide (CH_3I).

	VMR_{MABL} [ppt]	VMR_{ODR} [ppt]	VMR_{CLR} [ppt]	VMR_{ADR} [ppt]	$Flux_{MABL\text{-}FT}$ [pmol m^{-2} h^{1}]
$CHBr_3$	2.08 ± 1.36	0.89 ± 1.12	−0.05 ± 0.04	1.18 ± 1.20	4240 ± 1889
CH_2Br_2	1.17 ± 0.19	0.25 ± 0.26	−0.01 ± 0.01	0.92 ± 0.27	2419 ± 929
CH_3I	0.39 ± 0.09	0.28 ± 0.40	−0.05 ± 0.03	0.14 ± 0.37	865 ± 373

ACPD
15, 17887–17943, 2015

Table 5. Correlation coefficients between wind speed and VSLS MABL mixing ratios (VMR_{MABL}), the Oceanic Delivery (OD), the COnvective Loss to the FT (COL), the Advective Delivery (AD), computed as the residual of OD, and the mixing ratios originating from the OD (VMR_{ODR}) and from the AD (VMR_{ADR}). Bold numbers are significant at the 95 % (p value).

Wind speed	Bromoform	Dibromomethane	Methyl iodide
VMR_{MABL}	**0.55**	**0.57**	**0.56**
OD	**0.31**	**0.48**	**0.52**
COL		**−0.33**	
AD	−0.04	0.06	**−0.28**
VMR_{ODR}	**0.52**	**0.72**	**0.62**
VMR_{ADR}	−0.21	**−0.32**	**−0.53**

Table A1. As Table 3 and Table 4 using ERA-Interim MABL height.

	OD [% day^{-1}]	COL [% day^{-1}]	CL [% day^{-1}]	AD [% day^{-1}]	ODR	CLR	ADR	VMR_{ODR} [ppt]	VMR_{CLR} [ppt]	VMR_{ADR} [ppt]	MABL-FT Flux [pmol m^{-2} h^{1}]
$CHBr_3$	87.0 ± 124.5	−224.9 ± 70.7	−6.6	144.5 ± 143.1	0.43 ± 0.56	−0.03 ± 0.01	0.60 ± 0.55	0.88 ± 1.18	−0.07 ± 0.04	1.24 ± 1.20	4251 ± 1907
CH_2Br_2	39.3 ± 40.3	−224.9 ± 70.7	−1.8	187.4 ± 83.2	0.20 ± 0.21	−0.01 ± 0.00	0.81 ± 0.21	0.24 ± 0.26	−0.01 ± 0.00	0.93 ± 0.27	2456 ± 921
CH_3I	135.2 ± 195.0	−224.9 ± 70.7	−30.7	120.4 ± 220.8	0.73 ± 1.06	−0.15 ± 0.05	0.42 ± 1.03	0.28 ± 0.39	−0.06 ± 0.03	0.15 ± 0.37	799 ± 356

ACPD
15, 17887–17943, 2015
The contribution of oceanic halocarbons to marine and free troposphere air
S. Fuhlbrügge et al.

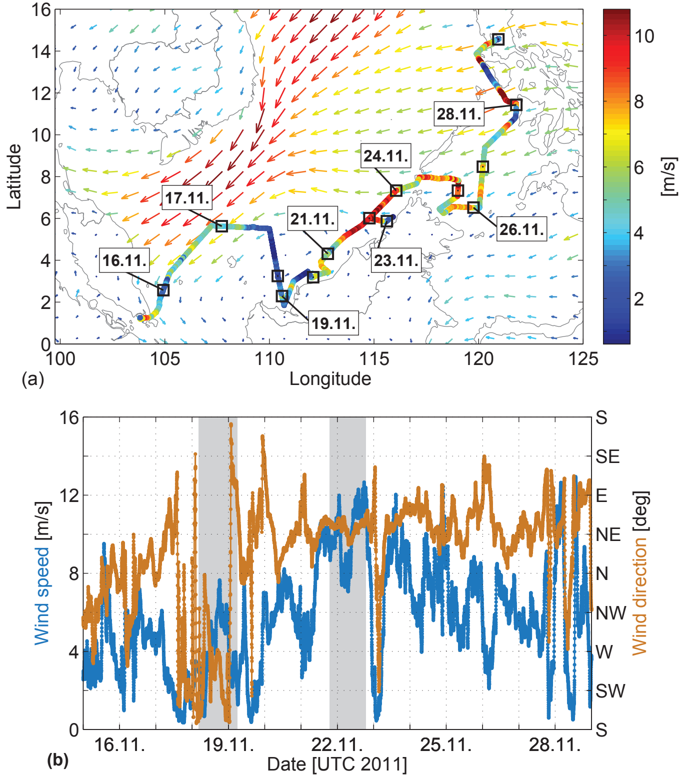

Figure 1. (a) ERA-Interim mean wind field 15–30 November 2011 (arrows) and 10 min running mean of wind speed observed on R/V *SONNE* as the cruise track. The black squares show the ships position at 00:00 UTC each day. **(b)** Time series of wind speed (blue) and wind direction (ocher) measured on R/V *SONNE*. The data are averaged by a 10 min running mean. The two shaded areas (light grey) in the background show the 24 h stations.

ACPD
15, 17887–17943, 2015

The contribution of oceanic halocarbons to marine and free troposphere air

S. Fuhlbrügge et al.

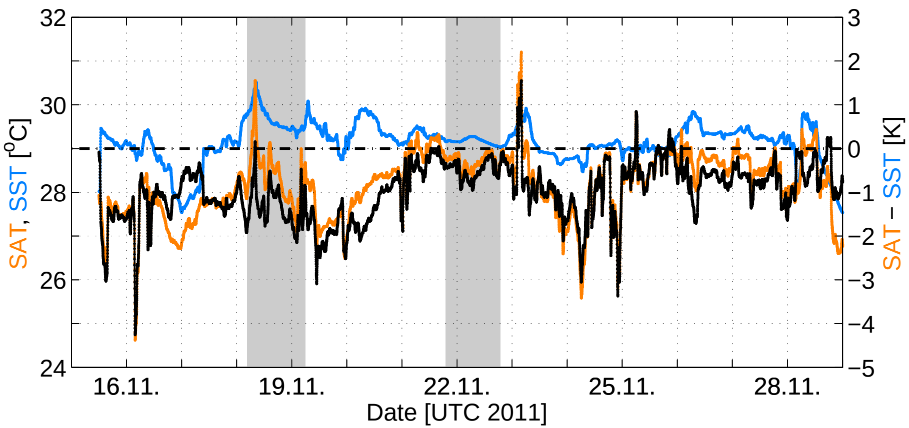

Figure 2. Time series of SAT (10 min running mean, orange) and SST (10 min running mean, blue) on the left and the difference of SAT and SST (10 min running mean, right scale). For the temperature difference, the 0 K line is given by dashed line. The two shaded areas (light grey) in the background show the 24 h stations.

ACPD
15, 17887–17943, 2015

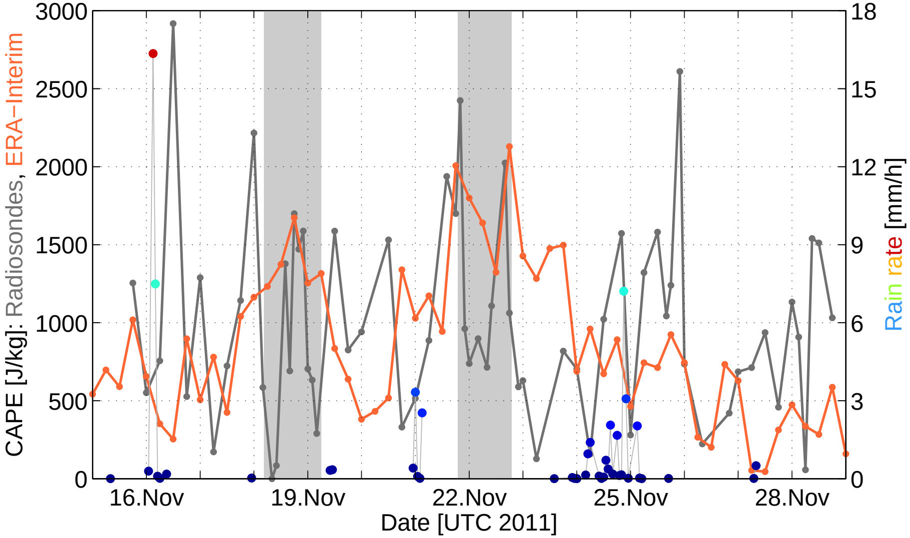

Figure 3. Left scale: convective available potential energy (CAPE) from radiosondes on R/V *SONNE* (grey) and ERA-Interim (orange). Right scale: Rain rate (colored dots) during the cruise, observed by an optical disdrometer (ODM 470) on R/V *SONNE*. The two shaded areas (light grey) in the background show the 24 h stations.

ACPD
15, 17887–17943, 2015

The contribution of oceanic halocarbons to marine and free troposphere air

S. Fuhlbrügge et al.

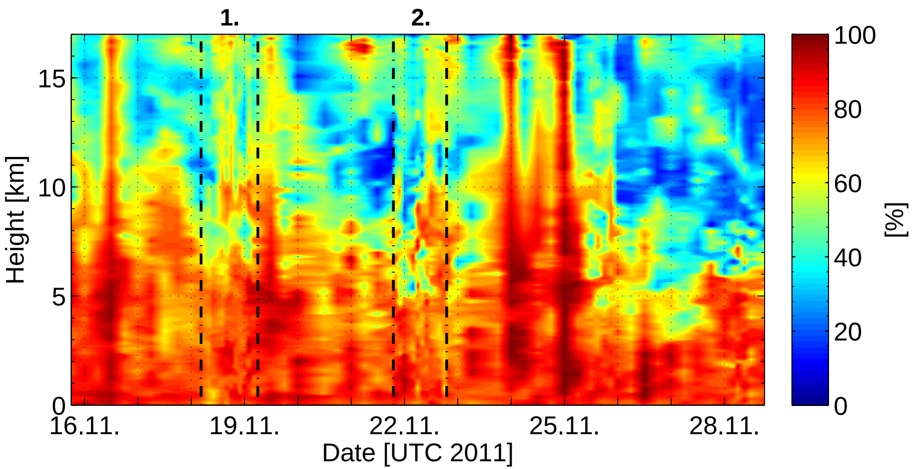

Figure 4. Relative humidity by radiosondes up to 17 km height, the mean cold point tropopause level. The dashed lines and the two numbers above the figure indicate the two 24 h stations.

ACPD
15, 17887–17943, 2015

The contribution of oceanic halocarbons to marine and free troposphere air

S. Fuhlbrügge et al.

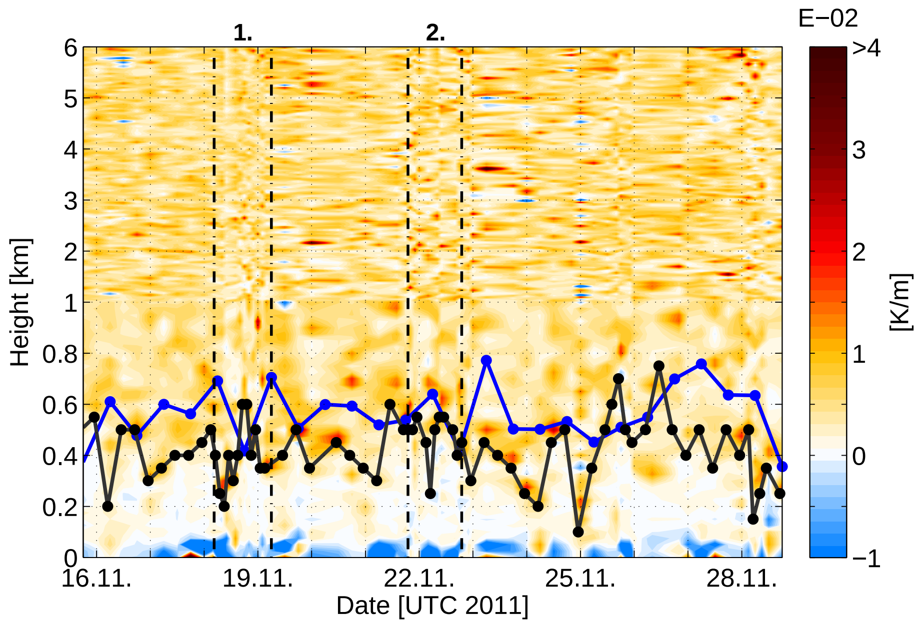

Figure 5. Virtual potential temperature gradient as indicator for atmospheric stability (red for stable, white for neutral and blue for unstable) with MABL height from radiosondes (black curve) and from ERA-Interim (blue curve). The *y* axis is non-linear. The lower 1 km is enlarged to display the stability around the MABL height. The dashed lines and the two numbers above the figure indicate the two 24 h stations.

ACPD
15, 17887–17943, 2015

The contribution of oceanic halocarbons to marine and free troposphere air

S. Fuhlbrügge et al.

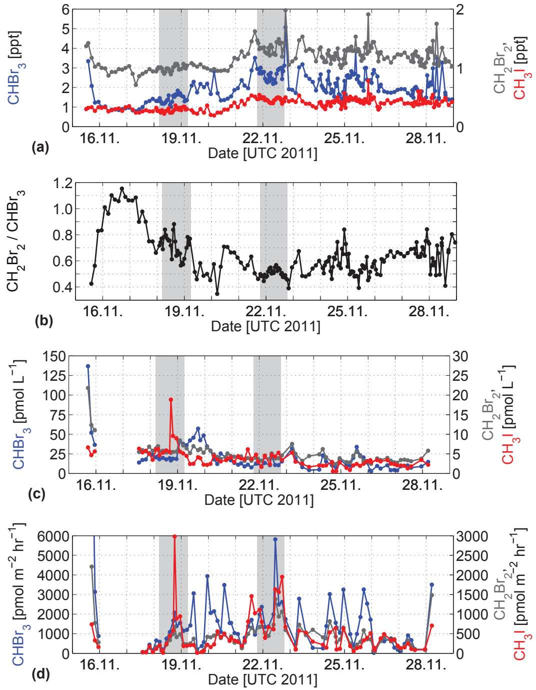

Figure 6. (a) Atmospheric mixing ratios of bromoform ($CHBr_3$, blue), dibromomethane (CH_2Br_2, dark grey) and methyl iodide (CH_3I, red) measured on R/V *SONNE*. **(b)** Concentration ratio of dibromomethane and bromoform on R/V *SONNE*. **(c)** Water concentrations of methyl iodide, bromoform and dibromomethane measured on R/V *SONNE*. **(d)** Emissions of methyl iodide, bromoform and dibromomethane from atmospheric and water samples measured on R/V *SONNE*. The two shaded areas (light grey) in the background show the 24 h stations.

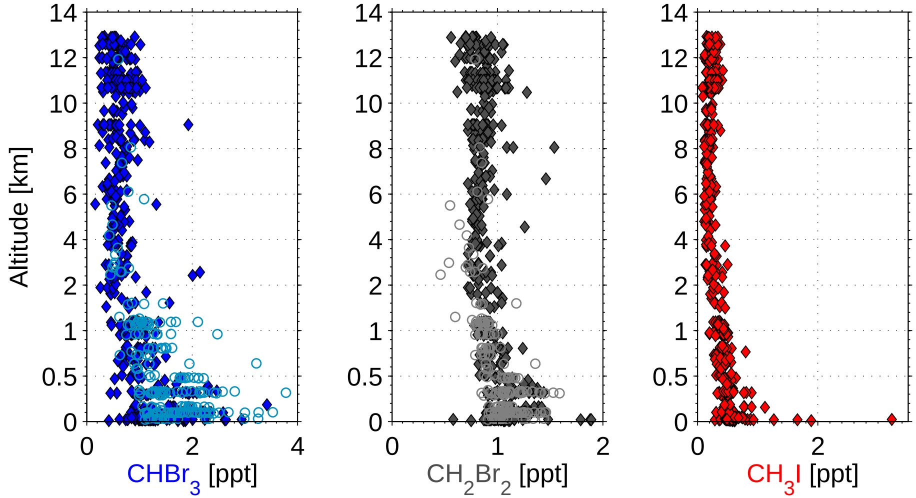

Figure 7. Vertical distribution bromoform ($CHBr_3$, blue), dibromomethane (CH_2Br_2, grey) and methyl iodide (CH_3I, red) mixing ratios measured by GhOST (diamonds) and WASP (circles) on R/A *FALCON*. Methyl iodide was only measured by GhOST. The lower 2 km are non-linear displayed.

ACPD
15, 17887–17943, 2015

The contribution of oceanic halocarbons to marine and free troposphere air

S. Fuhlbrügge et al.

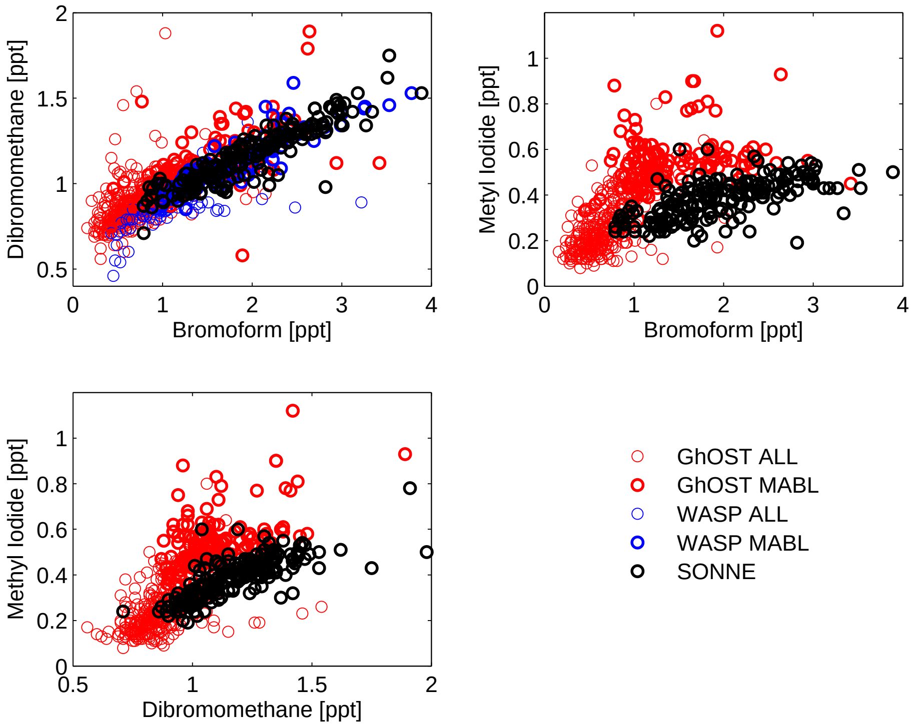

Figure 8. Correlation of bromoform and dibromomethane (upper left), bromoform and methyl iodide (upper right), and dibromomethane and methyl iodide (lower left) from GhOST and WASP for all heights (ALL) and only within the MABL (MABL) and from R/V *SONNE*.

ACPD
15, 17887–17943, 2015

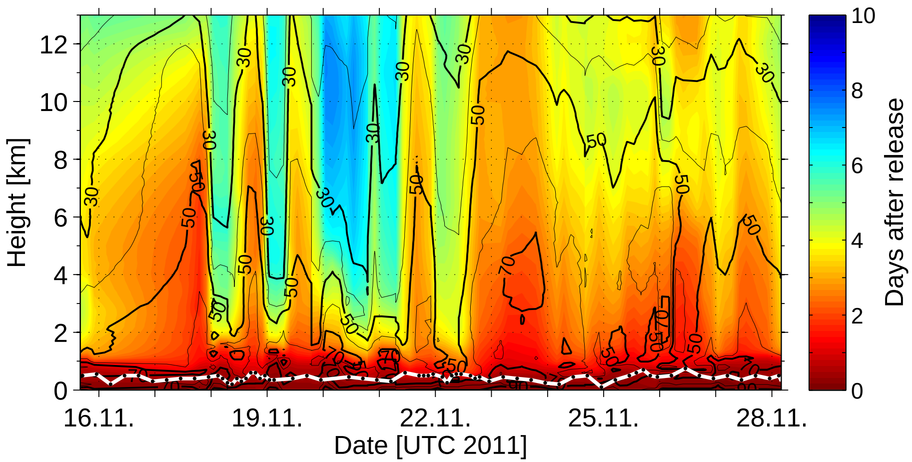

Figure 9. Forward trajectory runs along the cruise track with FLEXPART using ERA-Interim data. The black contour lines show the mean amount of trajectories (in %) reaching this height within the specific time (colour shading). The white line indicates the radiosonde MABL height.

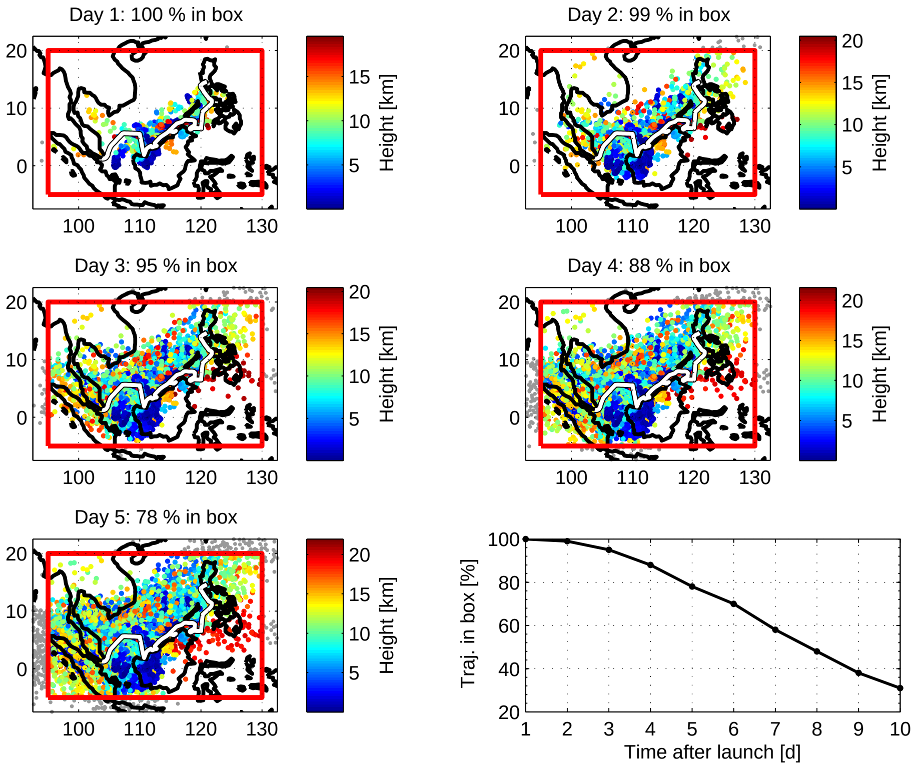

Figure 10. Horizontal distribution, altitude and amount of trajectories with time during the cruise. The red box represents the South China and Sulu Seas area. The lower right plot shows the amount of trajectories that remain in the box with time from all trajectory releases.

ACPD
15, 17887–17943, 2015

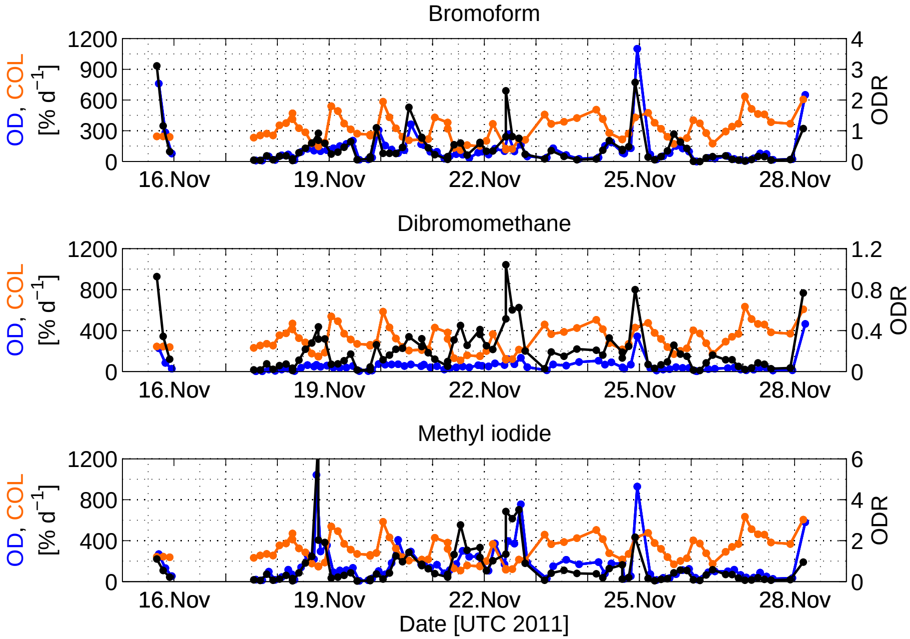

Figure 11. Time series of oceanic delivery (OD) to MABL concentration in % day^{-1} (blue), COnvective Loss (COL) from the MABL to the FT in % day^{-1} (orange) and the Oceanic Delivery Ratio (ODR, black) for bromoform (upper plot), dibromomethane (centre plot) and methyl iodide (lower plot).

ACPD
15, 17887–17943, 2015

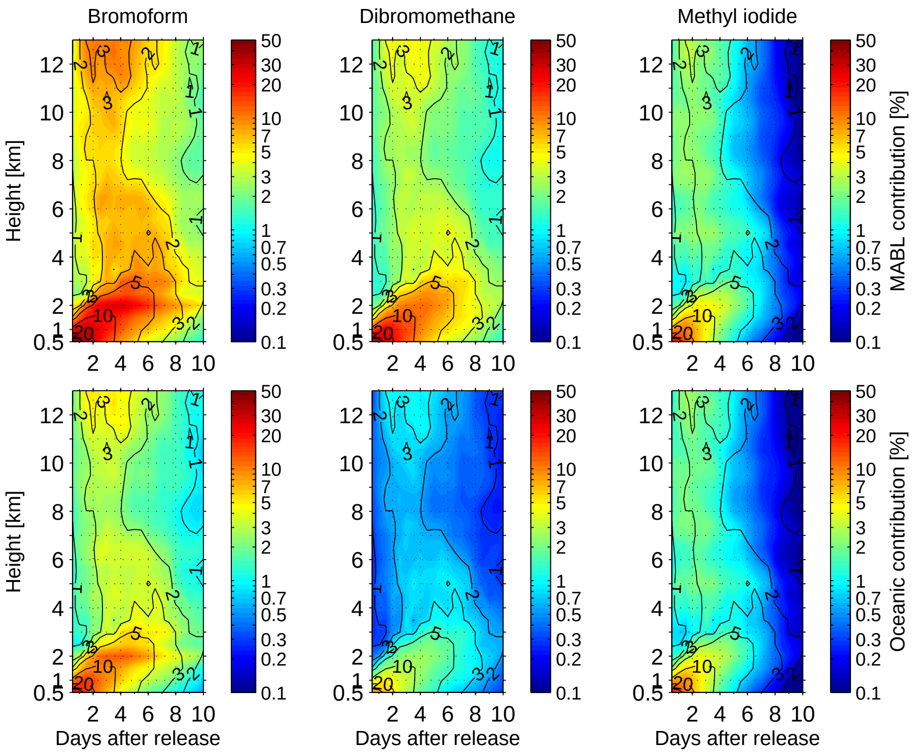

Figure 12. Mean MABL air contribution (upper plots) and oceanic contribution (lower plots) to observed FT mixing ratios observed by R/A *FALCON* for three VSLS. The black contour lines show the mean portion of MABL air masses in the FT [%], the colours show the oceanic contribution to the observed compounds in the FT, at specific height and day after release [%] including chemical degradation, the loss out of the South China Sea area with time and the vertical density driven extension of MABL air masses. The scale of the coloured contour is logarithmic.

ACPD
15, 17887–17943, 2015

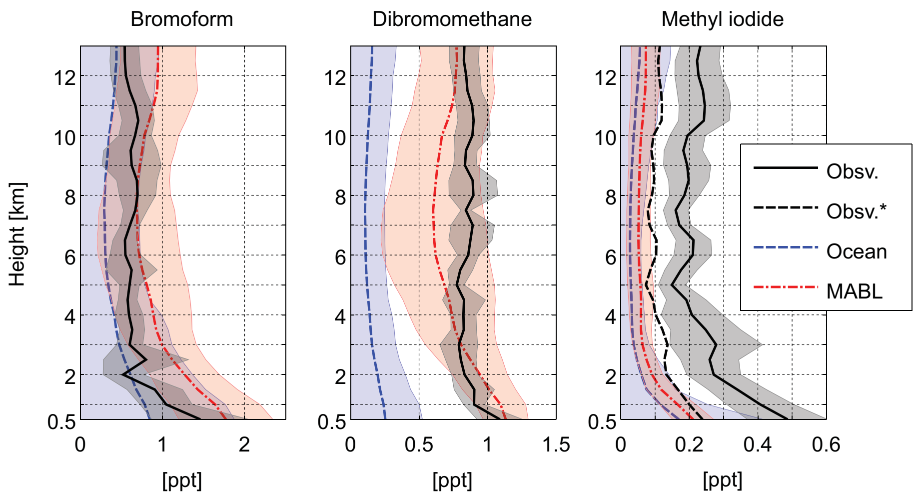

Figure 13. Mean FT mixing ratios (solid lines) and 1 standard deviation (shaded areas) observed by R/A *FALCON* (Obsv., black) vs. simulated mean FT mixing ratios from MABL air (MABL, red) and oceanic emissions (Ocean, blue) observed by R/V *SONNE*. R/A *FALCON* observations have been adjusted for methyl iodide (Obsv.*, dashed black) according measurements deviations during the meetings of R/V *SONNE* and R/A *FALCON* (compare Table 2; Sect. 4.3).

ACPD
15, 17887–17943, 2015

The contribution of oceanic halocarbons to marine and free troposphere air

S. Fuhlbrügge et al.